MASTERARBEIT | MASTER'S THESIS

Titel | Title

Engineering novel PEGDA hydrogels for reconstructing an artificial bone niche – a low-cost bioengineering approach

verfasst von | submitted by

Vinzenz Ambros Wöran BSc

angestrebter akademischer Grad | in partial fulfilment of the requirements for the degree of

Master of Science (MSc)

Wien | Vienna, 2024

Studienkennzahl lt. Studienblatt | Degree programme code as it appears on the student record sheet:	UA 066 877
Studienrichtung lt. Studienblatt | Degree programme as it appears on the student record sheet:	Masterstudium Genetik und Entwicklungsbiologie
Betreut von | Supervisor:	Univ.- Prof. Dr. Günter Lepperdinger

Table of Content

Acknowledgment

I would like to express my sincerest gratitude to Prof. Dr. Günter Lepperdinger for his guidance, endless support, his acceptance to work within his working group and to supervise my master thesis under his name. I further want to thank him for his input and countless ideas, which motivated me throughout the whole year and thought me to think in an experimental fashion.

Furthermore, I want to thank Andreas Struber MSc. for his constant support, his assistance and technical expertise, which greatly impacted this study. To all my colleagues, thank you for making this time pleasant and the best I could have wished for.

To Prof. Dr. Robert Konrad, thank you for taking charge and facilitating this master thesis at the University of Salzburg.

Finally, I want to express my gratitude to my parents and my family for the continuous and endless support throughout all these years.

Zusammenfassung

Die Entwicklung von synthetisch erzeugten Geweben und Organen ist ein intensiv behandeltes Thema in der modernen experimentellen Biomedizin. Es bietet nicht nur Einblicke in die Entstehung von Geweben, sondern versucht auch, alternative Wege für therapeutische Ansätze zur Behandlung von körperlichen Beeinträchtigungen und Funktionsstörungen zu entwickeln. Außerdem wird versucht, einen funktionelle Gewebeersatz herzustellen, um eine rasche Hilfe nach chirurgischen Eingriffen bieten zu können. Insbesondere im Bereich der Knochenrekonstruktion wird intensiv an der Entwicklung von Hydrogelen und Zell-Gerüsten gearbeitet, die die Regenerations- und Entwicklungsprozesse von Knochen verbessern und beschleunigen können. Parallel dazu bieten Lab-on-Chip-Anwendungen neuartige Möglichkeiten, 2D- und 3D-Zellkulturen einzubeziehen, um ein besseres Verständnis der Entwicklung von Organoiden und Organ-ähnlichen Strukturen zu ermöglichen.

Durch das Aufkommen kostengünstiger additiver Fertigungstechniken (Additive Manufacturing) kommt es gegenwärtig zu einem stetigen Fortschritt in der Entwicklung von mikrofluidischen Systemen, die für Anwendungen im Zusammenhang mit der Zellkultivierung und der Gewebeentwicklung eingesetzt werden können. Diese Verfahrenstechniken können durch schnelles und kostengünstiges Prototypisieren rasch an unterschiedliche Einflüsse angepasst werden, und bietet ein vielversprechendes Fundament für die Entwicklung in der Gewebeforschung.

Unter der Leitung von Günter Lepperdinger an der Universität Salzburg haben wir einen Ansatz zur Herstellung von Hydrogelen aus Polyethylenglykol Diacrylat (PEGDA) und Hydroxyapatit (HA) für Zellkultur-spezifische Anwendungen entwickelt. Wir haben den Einfluss von Hartgewebestrukturen auf HA-Basis auf Osteoblasten-Sphäroide nachweisen können und gezeigt, dass es zu einer Differenzierung und Mineralisierung der Zellen auf HA-Hydrogelen kommen kann.

Diese Masterarbeit stellt die ersten Versuche dar, 3D-Zellkultur in selbst produzierten mikrofluidischen Systemen zu etablieren. Darüber hinaus konzentrierte sich die Studie auf die Analyse und Prüfung verschiedener Materialien für künftige biotechnologische Anwendungen, um die Menge an Kunststoff in der Zellkultur zu reduzieren.

1. Abstract

Tissue engineering is an intensely covered topic in modern experimental biomedicine. It not only provides insight into the development of tissues but attempts to offer alternative ways of therapeutic approaches to manage disabilities, dysfunctions as well as offering solutions for functional tissue replacements after surgical removal. Especially in bone reconstruction, extensive work is undertaken to refine hydrogels and scaffolds that improve and expedite bone regeneration and maturation processes. In parallel and addition to that, lab-on-chip applications provide novel means to incorporate 2D and 3D cell culture approaches to facilitate a more profound comprehension of organoid-like growth and development. The emergence of low-cost additive manufacturing (AM) techniques currently promotes the development of microfluidic systems for application in the context of cell cultivation, drug testing and tissue development. Combining hydrogels in microfluidic systems is generally believed to better mimic in vivo-like conditions, potentially driving a steady progress in tissue engineering research. Genuine methods can be rapidly adapted to expedite the prototyping process. Under the supervision of Günter Lepperdinger at the University of Salzburg, we have developed an approach for manufacturing hydrogels made of polyethylene glycol diacrylate (PEGDA) and hydroxyapatite (HA) for use cell culture-specific applications. We have demonstrated the influence of HA-based hard tissue structure on osteoblast spheroids and whether differentiation and mineralisation of the structures have occurred. Initial attempts to develop microfluidic systems for 2D cell culture have also yielded promising results, suggesting the potential for combining AM applications with hydrogels in further research.

This master's thesis represents the first attempts at producing 3D cell culture on hydrogels in a cost-efficient, rapid and versatile manner, primarily for incorporation in an AM-produced microfluidic system. Furthermore, the study focused on analysing and testing several materials for future biotechnological applications to reduce the amount of non-sustainable plastic consumable in the cell culture lab.

2. Introduction

Since the development of the first microfluid systems in the 1990s, the number of annual publications has risen sharply. Microfluid systems, commonly known as lab-on-chip (LOC), offer a steadily increasing options of applications including also cell culture-specific experiments. These applications range from 2D over 3D cell culture to multiphysiological systems. It allows to pursue analysis on a single cell level, proteins, multidrug resistance, drug toxicity, tissue engineering and many more [1]. In particular, the continuing development of novel biocompatible materials together with affordable fabrication methods and equipment have greatly simplified prototyping in recent years, and now offers also non-specialized labs access to microfluidic systems [2-4].

Additive manufacturing (AM) describes the production and processing of materials using various crafting methods. AM is used in aerospace, automotive and marine industries. It also plays an essential role in biomedicine and has a wide range of application ranging from making implants, prostheses and medical models to manufacturing biomedical devices for tissue engineering. Especially in the medical field, it offers excellent potential for personalised and individually adapted applications [5]. In particular, the development of inexpensive and readily available 3D printers has played a significant part in the evolution of LOC [2, 3].

Microfluidic systems have been developed almost exclusively from polydimethylsiloxane (PDMS). Due to its excellent properties in terms of biocompatibility, gas permeability, cost-effectiveness, microchannel formation and elasticity, it can be applied in a wide range of applications [3, 6]. However, its production is very time-consuming and simple prototyping and fast adaptations are sophisticated. Furthermore, stable structures cannot be produced, and bonding with other materials is difficult or impossible. Channel deformation and leaching of uncured chemicals over time can affect cells and must also be taken into consideration. [3]. These aspects show that alternatives are needed to advance the development of LOCs.

With the further development of AM methods and the affordable solutions for the general public, previously rejected materials may reappear to the foreground as these may offer favourable properties. Hence, many microfluid systems are now made from polymethyl methacrylate (PMMA), cycloolefin copolymer (COC), polystyrene (PS), polylactide (PLA) or polyethylene glycol diacrylate (PEGDA) [1-3, 6, 7].

Thermoplastics such as PMMA, COC, PS and PLA are increasingly preferred due to their rapid, straightforward and highly cost-effective prototyping capabilities [3]. Using

computer-aided design (CAD) software, fluid chip designs can be drawn and visualised in three dimensions in no time. In this way, it is possible to react quickly and precisely to problems that arise, and, compared to soft lithography (e.g. PDMS), it provides efficient and cost-effective means for rapid prototyping. However, some materials (PMMA, COC, PS) show deficiencies concerning biocompatibility, and the production from fossil-based materials is no longer future-oriented. Conversely, PLA impresses with its good cell culture compatibility and cost-effectiveness. PLA is one of the most commonly used materials in the 3D filament printer sector, and conventional 3D printers are able to use it. In addition, PLA is derived from renewable resources and is environmentally friendly [3]. Due to the extensive market presence, significant developmental efforts are being done in this sector. Furthermore, the first transparent PLA filaments are already available on the market, but they must prove their value in developing transparent LOCs. PLA has the potential to emerge as a pioneering material with versatile applications.

An essential role in this master's thesis was using renewable resources, ecologically degradable products, and cost-effective materials to develop straightforward microfluidic systems. Furthermore, an attempt was made to use conventional materials and adhesives commonly encountered in everyday life. In the process, I addressed whether and how it would be possible to develop an inexpensive microfluid system for cell cultivation that anyone can assemble and manufacture in a short time, creating an alternative to classical cell culture.

When developing microfluid systems, the primary concern revolves around the selection of suitable materials for the intended application and their impact on cell culture. Silicones, which have become established in the past, are frequently used for this purpose. Due to the constant development of AM methods, choosing from a continuously growing range of materials is possible [3, 5]. Nonetheless, these materials must undergo toxicity testing to keep the error source low and counteract possible rejection. For toxicity and transplantation testings, the hen's egg test chorioallantoic membrane (HET-CAM) assay is an established method. While this test is extensively used in the development of implants due to its high sensitivity, simplicity and ease of execution, this method is usually too complex to test simple microfluidic systems [2]. Meaningful results can be obtained by utilising highly sensitive cell lines such as stem cells. We therefore established a method to gain reasonable results within three to four days to drive a developmental process. Here, the post-treatment after printing plays an

important role. Following sterilisation and washing, the device was conditioned in culture medium for 24 hours. In this way, potentially toxic chemicals are washed out. A clear result can be obtained after only two to three days through the contact of sensitive cells, like human fetal osteoblasts 1.19 (hFOB), with the conditioned material [2, 8].

A substantial part of my master's thesis was prototyping and cytocompatibility analysis of materials. Additionally, better understanding and solutions regarding material adhesion and bonding was projected. Many composites showed poor adhesion in humid environments, and the overall handling was often demanding.

Oxygen plasma bonding is a frequently used technique for bonding silicone to glass and altering the overall surface characteristics of materials. This process induces the formation of reactive groups and free radicals on surfaces, leading to an increased surface roughness and hydrophilicity of the materials [9]. Numerous studies have demonstrated that plasma treatments can also promote cell adhesion and are thus also applied to adapt microfluidic devices for cell cultivation [6, 7].

Even a brief treatment is already sufficient to make materials adherent for cells. This offers membranes and hydrogels, particularly an additional property and is highly advantageous in tissue engineering. Furthermore, newly conceived materials can counteract the immense plastic consumption in cell culture. When treated with plasma, PEGDA and cellulose hydrate acquire similar cell-adhesive properties to PS used in conventional cell culture dishes [6, 7]. Especially cellophane, the conventional name of cellulose hydrate, has great potential to being applied in cell culture as a low-cost and biodegradable alternative to fossil-based plastic.

Hydrogels have become indispensable in the biomedical field. They are instrumental in the development and success of tissue engineering and play an essential role in reconstructing tissues, bones and organs [10]. In particular, they are widely used to promote bone formation and support reconstruction [10-12]. Osteosarcoma, a prevalent form of bone cancer in humans, is frequently treated through a combination of chemotherapy and surgery [13]. This treatment involves removing defective bone structures to be subsequently replaced by autograft or allograft procedures. However, this often results in immunological rejection or inflammation, while autonomous bone healing is either too slow or limited [10, 11, 13-15].

Moreover, conditions such as osteoporosis, autoimmune and allergic diseases are associated with bone metabolism and are very common [16]. Therefore, studying the bone microenvironment is imperative, and research on suitable hydrogels for bone

repair and regeneration needs to be further advanced. These simulating bone scaffolds can increase bone mass by providing structural support and enhancing cell attachment and proliferation. Furthermore, due to their biocompatibility, they can be utilised in cell culture and implantation experiments [14]. Additionally, hydrogels are already harnessed as a drug delivery and cell carrier system to alter or enhance tissue development in particular areas [12]. Through this approach, bone reconstruction can be supported, and functionality regained, thus enabling the implementation of site-specific treatments.

Through the development of hydrophilic hydrogel materials, 3D network structures very similar to soft tissues are emerging. Hydrogels combine characteristics such as softness, stability, high permeability, elasticity and the ability to swell in water, facilitating the simulation tissue-like structures [10, 12].

Hydrogels, such as PEGDA exist that offer a quick and easy adaption in the structure by changing the molecular weight of the monomer. In addition to the molecular weight, the need and presence of photoinitiators play an essential role. Monomers or macromers can polymerise into polymers through UV irradiation, resulting in the formation of a 3D polymer network through the action of photoinitiators. The initiation of photopolymerisation via free radicals offers a fast method to manufacture hydrogels in diverse compositions and thicknesses [12]. PEGDA, with a molecular weight (MW) of 250, forms a stable and rigid structure that is applied to fabricate microfluidic chips or cell culture tools [6, 7]. Conversely, PEGDA 700 forms extended soft gel-like scaffolds that can be used for 3D cell culture and tissue engineering. Halim et al. described five properties to be considered in the context of bone scaffolds, including biocompatibility, surface quality to allow cell growth, mechanical robustness, a porous 3D network and biodegradable materials, all of which are necessary to achieve favourable outcomes [17].

To provide stable structures and niches for cells or tissues, additives such as hydroxyapatite [10, 14], chitosan [13], or laponite [11] have been incorporated into the hydrogel monomer to develop niches after polymerisation that control cell proliferation, cell attachment and differentiation [14].

Hydroxyapatite (HA) is an inorganic mineral extensively employed in tissue engineering as a bone substitute. It is fabricated synthetically and is also present in bone cells. In the human body, HA is found in bone, dentin and 95% of tooth enamel [13, 15]. Synthetic HA demonstrates biocompatibility and stability and can enhance osteoblast

proliferation and cell adhesion [14]. Additionally, it serves as an osteoinductive promoter of osteoblastogenic genes such as alp, runx2 and col1 [18]. Osteoblasts play a crucial role in bone mineralisation, responsible for the production of HA and the mineralisation of extracellular matrix, which leads to ossification of the cellular environment [19]. Extracellular matrix is formed on the surface of osteoblasts, in which large amounts of intracellular calcium and extracellular phosphate form HA crystals. Alkaline phosphatase (ALP) is an essential protein in this differentiation process. Its expression is regulated by multiple signalling pathways, such as Wnt, BMP2, FGF and many more, and significantly influences mineralisation. It hydrolyses existing pyrophosphate to inorganic phosphate (Pi). Since inorganic pyrophosphate (PPi) acts as an inhibitor of HA formation, a balance between Pi and PPi is crucial for mineralisation. However, the exact mechanism of ALP expression is very complex, but for analysing purposes, it works as an indicator for mineralisation [19].
Several studies have demonstrated that HA can improve and accelerate bone reconstruction. The combination of HA with hydrogels, such as PEGDA, has shown promising outcomes in bone regeneration [10, 11]. An important point is to induce osteogenesis to drive differentiation. Liu et al. have illustrated that PEGDA/HA membranes can enhance bone growth and regeneration in rats. The hydrogels were loaded with a regulator that augmented osteogenic efficiency and bone mass, serving as both a support scaffold and drug delivery system [10]. Other research groups have also shown promising results that may serve as a foundation for future investigations [10, 11, 14].

In an additional part of my master's thesis, I worked on developing hydrogels to detect osteogenic differentiation and mineralisation. In doing so, I examined the question whether there is a difference between osteoblast spheroids on HA and spheroids in typical cell cultures. The aim was to develop an economical and straightforward method for fabricating PEGDA/HA. We intended to design a system capable of analysing 2D and 3D hydrogel-based cell cultures within a microfluidic system over an extended period. We designed and engineered a pump system for the supply of nutrients over several days without disturbing microscopic observation. A future-oriented application has been developed by fusing 3D cell culture with microfluidic systems, which may hold great promise in tissue engineering due to its cost-effectiveness, ease of replication and operational simplicity.

3. Material and Methods

3.1. Cellular Biology

3.1.1. 2D Culture

For the experiments, the cell line human fetal osteoblasts 1.19 (hFOB, American Type Culture Collection, CRL-11372) was cultivated in a 100 mm tissue culture dish in Dulbeco's Modified Eagle Medium/Nutrient Mixture F-12 (DMEM/F12, Sigma-Aldrich, Taufkirchen, Germany; D6421), to which 10% fetal bovine serum (FBS, Cornig, COR-079), 1 % penicillin–streptomycin (Sigma-Aldrich, P4333), 1% L-Glutamine (Sigma, G7513) and Gentamicin 6mg/ml (G418, Sigma, G8168) was added.

The cells were incubated at 34°C and a CO_2 concentration of 5% until they reached a confluency of around 80-90%. For harvesting, the cells were washed with Dulbeco's Phosphate Buffered Saline (PBS, w/o Calcium, w/o Magnesium, ECB4004L) before they were exposed to Trypsin/EDTA (PBS solution containing 0,025% Trypsin and 0,01% EDTA) for 5 minutes. The cells were counted with a hemacytometer (Neubauer) and were stored on ice for further applications.

3.1.2. 3D Culture and Spheroid Formation

To form spheroids, U-bottom 96-well plates (Greiner) were first coated with sterile–filtered 3% pluronic F-127 (Sigma-Aldrich, P2443) and then washed three times with cold PBS. The plate was centrifuged at 300xg at 5°C for 5 minutes between each washing step. After preparation, cells were transferred to the plate at a concentration of 10^3 cells per well and incubated at 34°C and 5% CO_2 for 48 hours.

3.2. Biocompatibility Tests

Various materials were processed for cytocompatibility testing. For this purpose, they were either laser cut (Trotec Speedy 100), 3D printed with filament (Original Prusa i3 MK3), processed by stereolithography (Phrozen Sonic Mini 4K) or cured.

After preparation, the materials were sterilised with EtOH, H_2O_2 or UV, depending on their properties and compatibility. In general, the materials were sterilised for 30 minutes each. They were washed thrice with PBS before being conditioned with medium (DMEM/F12) for at least 24 hours.

Furthermore, the materials were transferred into 30 or 60-mm culture dishes, depending on size. Tissue culture dishes (Greiner) were used for materials to which cells should adhere to the bottom. Bacteria dishes (unknown) were used for membranes or other constructs, to which cells should preferably adhere to the materials themselves.

For the 30-mm dishes, a cell concentration of $3x10^5$ and for the 60-mm dishes, a concentration of $6x10^5$ was seeded to obtain confluency within two to three days. This enabled the utilisation of microscopic analysis to determine the cytotoxicity of the material or its suitability for incorporation into cell culture experiments.

3.3. Manufacturing of PEGDA – HA Membranes

Polyethylene Glycol Diacrylate (PEGDA, average molecular weight: 700, Sigma-Aldrich, 455008, Lot # MKCK7369) was mixed with 0,5% (w/w) Phenylbis (2,4,6-trimethylbenzoyl) phosphine oxide (Igarcure 819, Sigma-Aldrich, 511447, Lot # MKCJ3123) and 5% (w/w) HA (BIO-RAD, DNA Grade, Bio-Gel® HTP Gel, 130-0520). The receptacle was wrapped with aluminium foil to prevent premature curing. The hydrogel was blended within an ultrasonic bath for 10 minutes to obtain a homogenous solution.
For curing and laser cutting, a construction consisting of two 150x150mm glass plates was used to produce hydrogels. Cyclic olefin copolymer (COC) foil was taped to each glass slide for smooth membrane removal. Approximately 2-3 ml of the hydrogel was transferred onto one of the slides using a cut pipette tip before the second slide compressed the construct from above. To obtain a membrane thickness of 150-300 µm, the sandwich was squeezed with a foldback clip and placed in the UV chamber (LED Light Cure Box, 65W, Phrozen Cure, Taiwan) for ten minutes. The plates were separated using tweezers and a knife to remove the membrane from the foil. For further applications, the membrane was taped into a polymethylmethacrylate (PMMA) frame, placed in the laser cutter (Trotec Speedy 100) and calibrated to the Z-axis. Membranes of PEGDA 700 were cut out with a diameter of 28 mm, and non-hydrogel films, like COC or cellophane, were cut out as 35 mm circles.

3.4. Prototyping 2D and 3D constructs

The design of 2D drawings was created in the open-source software LibreCAD (GPLv2, version 2.2.0, 2022). Afterwards, the file was exported in the .dxf format and subsequently imported into CorelDraw (Corel, version 2022). Within CorelDraw, specific regions were marked for cutting or engraving. A print task was then initiated within CorelDraw and sent to JobControl (Trotec, version 11.4, 2023). Within JobControl, the parameters for the laser cutter were defined, and the laser cutter's operation was maintained. In Table 4, settings for different materials and membranes are listed. In order to be able to carve out holes in the 200 µm range (resolution limit of the laser cutter), the engraving function of the laser cutter was used.

The 3D designs were created using AutoCAD 2023 (Autodesk, version 24.2, 2022) and converted into .stl files. For 3D filament printing, the software PrusaSlicer (Prusa, version 2.6, 2023) and for stereolithography (SLA) printing, the software Chitubox (CHITUBOX, version 1.9.4, 2022) was used. Both software assembled appropriate G-codes from the .stl files and transferred them to the printers.

3.4.1. Prusa i3 MK3

For the filament 3D printer, the following settings were used: For Polylactic Acid (PLA, Velleman, ∅ 1,75mm, PLA175W07) prints, the heating plate was set at 60°C, the nozzle at 215°C for the first layer and 210°C for the remaining layers. For prints made of COC (Cremelt, 190521, ∅1.75mm), the temperature for the print board was set to 90°C and the print temperature for all layers was set to 250°C. Furthermore, in the case of material COC, an additional foil of COC or cellophane was taped on the base plate on which the design was printed.

For both printing materials, a layer height of 0,2mm was set.

3.4.2. Phrozen Sonic Mini 4K

The following settings were used for PEGDA 250 (average Mn: 250, Sigma-Aldrich, 475629) with 0,1% Irgacure 819 and PEGDA 700 with 1% Irgacure 819: the layer height was set to 0,05mm, the bottom layer count to 5, the exposure time to 5 seconds, and the bottom exposure time to 20 seconds.

3.4.3. Finalising prototyped Microfluid Systems

After printing, where necessary, holes (1-mm width) were drilled into the finished 3D print and roughened with sandpaper for further processing. The silicone tubes with a outer diameter of 1.0-1.3 mm were glued with epoxy glue (Toolcraft, 886519, purchased from conrad.at; or Presto Epoxy-resin 500g, purchased from OBI), and the membranes or bases were glued and pressed with double-sided adhesive tape (3M™, 7959MP). The microfluidic chip was then treated with oxygen-plasma before being prepared for cell culture.

After sterilisation, washing, and conditioning, $2x10^4$ cells were added to the opening of the chip. To avoid desiccation, the lid was tightly sealed with a foil (Microseal® B Adhesive Sealer, MSB-1001, Biorad), and the inlet and outlet tubes were closed with cannulas and syringes. Following a 24-hour incubation period at 34°C and 5% CO_2, the tubes were clamped into the reservoir and syringe pump system. Subsequently, the program with a flow rate of 2.5 µl/min was started. A continuous flow was set to

ensure a complete replacement, which replaced 3.7 ml (adjustable in Arduino code, Supplementary Protocol 8.2) of medium per 24 hours.

3.5. Cellophane Prototyping and Preparation for Cell Culture

Cellulose hydrate foil (purchased by Spar supermarket), commonly called cellophane, was manually cut or with the aid of a laser cutter (Table 4). When cellophane was used as a membrane for microfluid chips, the foil was either taped to the heating plate of the 3D printer, or cut out by laser cutter (Trotec Speedy 100) and applied to the surface of the printed chip using double-sided adhesive tape (3M). When the cellophane membrane was used as a stand-alone experiment, the film was soaked in dH_20 for 15 minutes, folded or formed into a shape and then pressed with a screw clamp for 15 minutes. This procedure forced the membrane to retain shape for at least 43 days. After preparation, the membrane was treated with plasma for 25 seconds, then sterilised for 30 minutes with EtOH (70%) and afterwards conditioned for 24 hours, as described below.

3.6. Plasma Treatment and Conditioning of Various Membranes

In order to achieve a uniform surface modification, the membranes were taped to a PMMA plate with Scotch tape. Upon positioning the plate in the plasma chamber (Diener electronic, O_2 Plasma chamber), the lid was closed, and the chamber evacuated. After reaching a 0.4-0.3 mbar vacuum, the chamber was flooded twice with pure oxygen (Air Liquide). Following a third time of vacuum, plasma was generated for 25 seconds. Afterwards, valves were opened until atmospheric pressure was set to open the enclosure. The membranes were quickly placed in EtOH (70%) for 30 minutes, washed thrice for 10 minutes with PBS, and then placed in the medium (DMEM/F12) for conditioning for 24 hours.

3.7. Cell Culture-specific Experiments on Hydrogels

6-well tissue culture dishes (Greiner) were first coated with 3% sterile filtered pluronic. The plasma-treated and conditioned membranes were carefully placed into the wells with tweezers before single cells (cell concentration 10^3) or spheroids (8 to 16 cell aggregates) were transferred onto the membranes, ensuring the presence of an appropriate volume of medium (DMEM/F12). The cells were incubated for 48 hours at 34°C and 5% CO_2 to ensure full adhesion.

For the medium replacement, the liquid was carefully taken up with a 200 µl pipette at the edge of the well. The same method was applied to fresh medium or PBS. To minimise the number of medium exchanges, two times the amount of medium, usually

used, was added to ensure cell viability for 3-4 days. In this way, transfer of the plates from the incubator to the cell culture hood is reduced, thereby minimising the potential of cell detachment.

3.8. Cell and Spheroid Staining

3.8.1. Fixation and Alkaline Phosphatase Staining

Since cells and spheroids need time to adhere to the membranes, the liquids were carefully aspirated at the edge of the wells with 200 µl pipettes. Spheroids, which were selected for control or alkaline phosphatase staining were fixed with 4% Paraformaldehyde (PFA) in each case.

For staining with alkaline phosphatase, the aggregates were washed once with PBS-Triton X-100 (0.1% Triton X-100) before being fixed with 4% PFA for 30 minutes. Subsequently, the PFA was withdrawn and neutralised three times with PBS for 10 minutes before being pre-treated with Alkaline Phosphate Buffer (APB, Supplementary Material 8.3) three times for 10 minutes. 15 mg/ml of the ALP dye NBT/BCIP (Boehringer Mannheim, nitro blue tetrazolium/ 5-bromo-4-chloro-3-indolyl-phosphate; Oct 1998, 14516825-04) was added to a vial containing sufficient APB to cover membranes and cells. The cells were incubated overnight at 34°C and 5% CO_2 and washed 3x for 15 minutes with dH_20 the next day.

3.8.2. Xylenol Orange Staining

For fluorescence staining with Xylenol Orange (XO, Fluka Analytiks, 83325, Lot #83290, live staining), the cells and aggregates were first washed once with PBS and stained with medium (DMEM/F12) containing 20 µM XO. Cells were incubated overnight at 34°C at 5% CO_2. Before microscopy acquisition, the dye was aspirated with a 200 µl pipette and washed 3x with PBS. Subsequently, the cells were provided with adequate DMEM (PAN Biotech, P04-01161, w/o Sodium pyruvate, w/o L-Glutamine, w/o Phenol red, with 4.5 g/L Glucose and with 3.7 g/L $NaHCO_3$) not to influence imaging.

3.9. Setup of the Syringe Pump System

The syringe pump comprised of the pumping mechanics along with the syringe assembly (components listed in supplementary material 8.4), as well as the input panel. A power supply unit (Sony, 19.5V, 4.7A) was used to supply enough power for the stepper motor driver. Furthermore, a USB power supply unit (unknown manufacturer, 5V output voltage) was employed to operate the Teensy 4.1 microcontroller. The supply cables were inserted into the labelled sockets. The 4-pin connector for the stepper

motor was also attached to the control panel. On the display screen, the pre-programmed options can be selected via the push buttons. Hence, a back button was integrated to exit the operating program and a return key to regain access to the main menu. Four buttons on the right side control the stepper motor in both ways with two different speeds. This function enabled the adjustment of the pump to respond to different sizes of syringes and other relevant parameters.

4. Results

4.1. Novel Biocompatible Materials for Microfluidic Prototyping

The microfluidic systems described in the literature are typically made of several layers [2, 3, 8, 16, 20, 21]. Bonding surfaces or sealing materials are often problematic, and searching for suitable materials is time-consuming. Furthermore, the appropriate material choice depends on the properties and field of application.

We tested many materials for sealing, as chip material, and as possible membranes for cell adhesion experiments. Our analysis focused primarily on cytocompatibility, cellular attachment and for the wide range of application in the microfluidic sector.

4.1.1. Materials for Microfluid Systems

For the cytocompatibility analysis, the human fetal osteoblasts (hFOB) 1.19 cell line was employed. Cell and material treatment was performed according to an approach from previously established in the research group [2]. Therefore, materials were sterilised with EtOH (except PMMA with H_2O_2), washed with PBS and conditioned in DMEM/F12 medium for at least 24 hours. The obtained outcomes are presented in Table 1:

The thermoplastics COC and PLA presented excellent cytocompatible properties, comparable to PDMS, dental impression material and PEGDA 250. However, surprisingly, we could not confirm the cytocompatibility for polymethacrylate (PMMA) and polytetrafluorethylene (Teflon) (Figure 1 A-B). Both appeared to be toxic and not usable for our applications. Especially PMMA, which has been used in the literature for countless microfluidic applications, clearly showed toxic effects on hFOB cells [2, 3, 8, 22]. Even after several washing steps, no positive result could be achieved.

Teflon is also often utilised in cell culture due to its hydrophobic properties, but similar poor results were obtained here.

These results may be due to the different compositions or the high sensitivity of the hFOB cells. Based on the excellent properties and biodegradability of cellulose hydrate

(Figure 1 D), a microfluidic chip made of compostable materials was designed. We used wood (spruce), buffalo horn and bones from deer antlers, but in natural form, only buffalo horn turned out to be suitable. As presented in Table 1, the wood was treated with different materials. A coating of printer's wax and epoxy glue proved to be promising. However, a fully compostable microfluidic system could not be developed because both the sealing of the materials and the adhesives for the membrane adhesion were unsuitable.

Materials: Chip	toxic	non toxic	slightly toxic
PDMS		x	
PMMA	x		
Teflon	x		
COC		x	
PLA		x	
Dental impression material		x	
PEGDA 250		x	
Wood (Spruce) untreated	x		
Wood (Spruce) cut	x		
Wood (Spruce) coated with PEGDA 250	x		
Wood (Spruce) coated with wood glue	x		
Wood (Spruce) coated with shellac	x		
Wood (Spruce) coated with printing wax		x	
Wood (Spruce) coated with linseed oil	x		
Wood (Spruce) coated with linseed firnis	x		
Wood (Spruce) coated with low-viscosity epoxy		x	
Buffalo horn		x	
Bone (Deer)			x

Table 1: Listing of Materials for Developing Microfluidic Devices

Another interesting material was dental impression mass. The results demonstrated favourable cytocompatibility and was amenable for moulding into different shapes during the curing phase. However, a negative aspect was its non-adhesive properties. Neither epoxy, double-sided tape, nor plasma bonding allowed possible adhesion of membranes, foils or glass. Buffalo horn exhibited a high degree of biocompatibility, and various adhesives showed favourable properties on the surface. The only challenge encountered in developing a possible compostable chip was that 3-5 mm horn plate could not be processed by laser cutting. While machining was possible, no equipment that would allow rapid prototyping was available. Bone from deer was also tested

for toxicity to develop possible microfluid chips from existing bone. However, the tests showed low toxicity and prolonged conditioning was not possible due to leaking fluids through the pores of bone material.

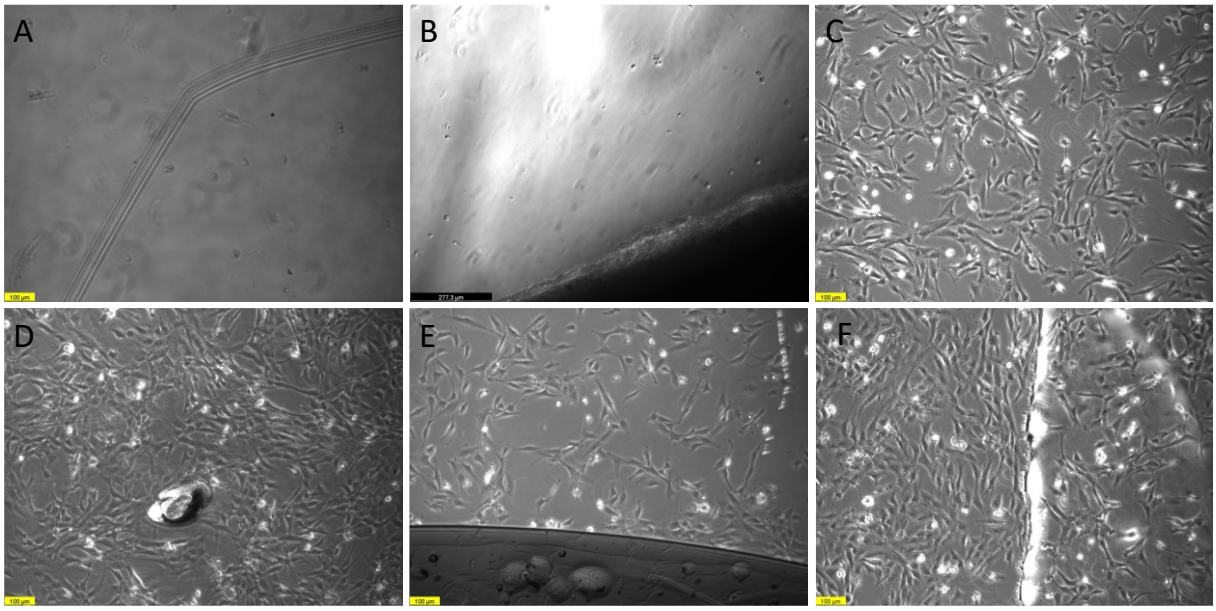

Figure 1: Microscopic images of cell cultivation of different materials potentially applicable for microfluidic devices. Cells (hFOB 1.19) with PMMA ***(A)*** *and Teflon* ***(B)*** *showed no viability after 3 days of cultivation. PLA* ***(C)****, Cellophane* ***(D)****, Epoxy* ***(E)****, and double-sided Tape* ***(F)*** *showed did not impinge on cell growth and proliferation. All images were captured on day three by Leica DMiL and using the LAS X Software (Leica).*

4.1.2. Materials for distinct Membranes and Hydrogels

The membranes and hydrogels listed in Table 2 appeared all suitable for cell culture-specific experiments. Figure 1 D depicts hFOB proliferation taking place on plasma-treated cellophane. Confluency was already detectable after two to three days. Compared to tissue culture dishes, no distinguishable differences in confluence was observed. In addition to the excellent adhesive properties of cellophane, the double-sided adhesive tape from 3M and both epoxy glues have been proven to be suitable substrates for cell adhesion experiments (Figure 1 E-F). For experiments that do not require cell adhesion, COC or BioRad foils also appear suitable. Both plasma and UV treatments did not change the surface properties of these two materials. Yet, we were not able to establish cell adhesion by this means.

Material: Membranes	toxic	non-toxic	Adhesive	non-adhesive	slightly adhesive
PEGDA 250, Plasma treated		x	X		
PEGDA250 + HA, Plasma treated		x		x	
PEGDA 700, Plasma treated		x		x	
PEGDA 700 + HA, Plasma treated		x	x		
PEGDA 700 + HA, 10h UV treated		x			x
Cellophane, Plasma treated		x	x		
COC-Foil		x		x	
BIORAD -Foil		x		x	
3M double-sided tape		x	x		
Epoxy		x	x		
Epoxy low viscosity		x	x		

Table 2: Listing of Membranes and Hydrogels useable for Cell Culture

The tests showed that we were able to produce thin cytocompatible hydrogel membranes from PEGDA 250 as well as from PEGDA 700 (Table 2). In all the experiments, the surfaces were treated with oxygen plasma. Only PEGDA 700 with HA was tested after a 10-hour UV treatment. As shown in Table 2, cells were able to adhere to pure PEGDA 250 as well as to PEGDA 700 + HA. Surprisingly, this was not achieved on PEGDA 250 with HA or pure PEGDA 700. However, with the wider-meshed hydrogel, the required hydrogel structure and bone-like substance were obtained for the desired prospective application.

Cell adherence was also achieved on PEGDA 700 with HA hydrogel after 10 hours of UV treatment. Nevertheless, it has been shown that the cells adhered more efficient after plasma treatment and when seeded over the entire membrane.

4.1.3. Adhesives for Bonding and Sealing

Since microfluidics often involve multiple layers, bonding and sealing techniques are relevant. Especially for PDMS, plasma bonding is very frequently applied [3, 16]. However, this treatment typically applies to only a limited selection of materials. Therefore, an evaluation of adhesives is necessary for designing microfluidic devices. We encountered the following conventional adhesives that have been investigated in this study (Table 3):

The results have shown that both epoxy glues and FixoGum can be used as adhesives for sealing silicon tubings while a secure and reliable seal could be achieved by complying the curing time prescribed by the manufacturer's specifications.
Similar results were achieved with FixoGum. FixoGum is a commercially available adhesive based on natural rubber and achieved excellent biocompatible properties in our analysis.
Surgibond, on the other hand, which is often referred to as a tissue glue, did not score well both regarding its adhesive strength or biocompatibility.
The double-sided adhesive tape produced by 3M™ and the foil from BioRad were excellent for bonding membranes or foils. They convinced with robust and secure adhesive strength and non-toxic properties. These two foils were also often used in the experiments as they could be quickly applied.

Material: Glue	toxic	non toxic	slightly toxic
Epoxy Glue		x	
Surgibond	x		
Fixo-Gum		x	
UHU-Creative			x
UHU-Superglue	x		
Silicone rubber	x		
3M™ double-sided tape		x	
BioRad -Foil		x	
Epoxy Glue (low viscosity)		x	

Table 3: Listing of glues that were used for sealing and bonding of materials

4.2. Cellophane Prototyping

Since the tests showed that cellophane has versatile and excellent properties for cell culture, an experiment was carried out to observe the development of 3D cell structures derived from John Dunlops work [23]. Therefore, wetted cellophane foil was folded by hand and then pressed with a screw clamp for 15 Minutes. After plasma treatment, sterilisation and conditioning using the above-mentioned method, the folded foil was placed in a 35-mm bacterial dish (Figure 2). Due to the transparency of the material and the cell adherence, cells (10^3 cells per dish) were placed on the foil and observed microscopically for 43 days.

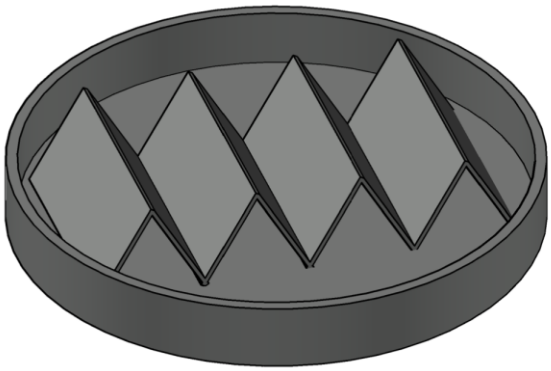

Figure 2: Illustrative model of the angled cellophane membrane in a bacteria dish designed with AutoCAD

The cells aligned along the groove in the first five days and proliferated. Already on the seventh day, first spheroids emerged on top of the confluent cellophane foil. Spheroids mainly formed on the steep flanks and moved towards the channel over time, and some of the spheroids joined together to form large constructs. After 15 days, some spheroids could already be observed in the grooves, but due to the steep flanks and the poor microscopic analysis, no clear interpretation could be drawn concerning the formation of further 3D cell layers. A limiting factor was the angled membrane, which was challenging to focus on, making a possible layer-specific analysis difficult. Microscopic images of the described experiment can be seen in Figure 3.

After 43 days, the experiment was terminated as a large cell lawn had formed, which made microscopic observation significantly more challenging.

This observation shows that spheroid formation and especially 2D cell culture can be encountered and monitored on cellophane foils.

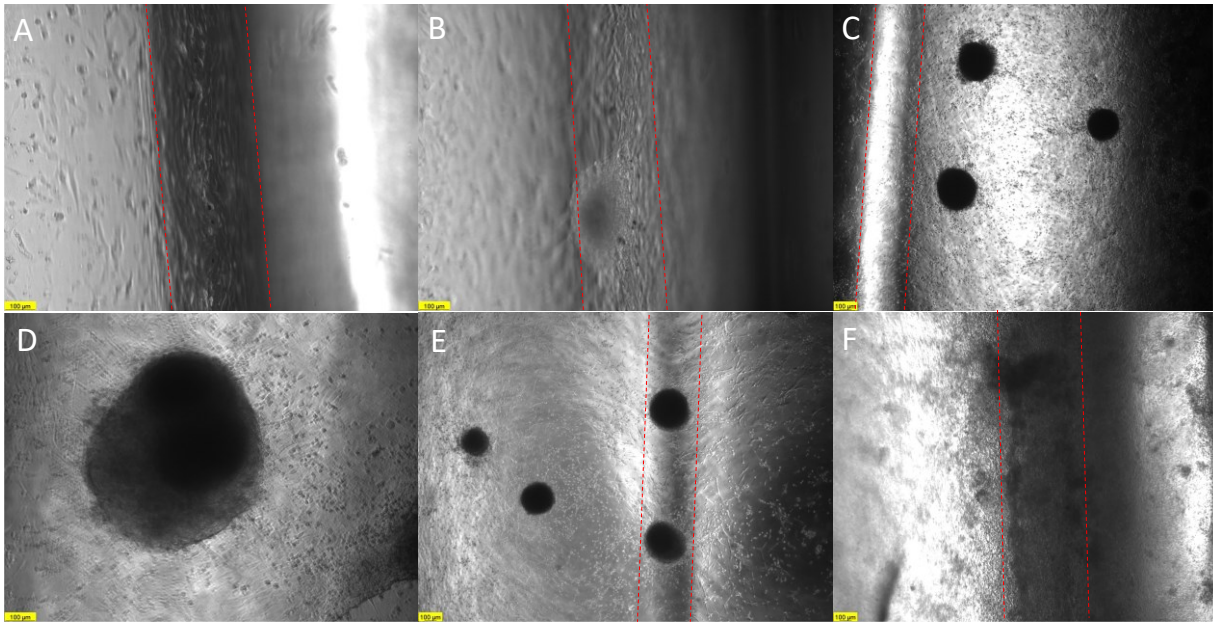

Figure 3: Cells seeded on the folded plasma-treated cellophane foil. ***(A):*** *on day five, cells proliferated around the foil and aligned in the groove of the foil, cellophane membrane confluent.* ***(B):*** *first cell aggregates were formed on day seven.* ***(C):*** *spheroids were mostly formed on the steep flanks (day 12) and often aggregated together* ***(D,***

*day 14**). (E):** on day 20, visible migration of spheroids into the groove. **(F):** massive cell lawn around the membrane, especially around the grooves but no visual differentiation possible (day 43). The red lines indicate the grooves. All images were captured on Leica DMiL using the LAS X Software (Leica).*

4.3. Manufacturing of PEGDA 700 + HA Hydrogel Membranes

Different approaches as to produce hydrogels have been established. Thin discs and other constructs can be realised with the help of SLA printers, mainly using complex techniques. [6] The limiting factors for designing and producing hydrogel membranes are the SLA printer's resolution, the polymers' cross-linking, and the photoinitiator. In this study, a straightforward and cost-effective method to assemble hydrogel membranes with reduced photoinitiator Irgacure 819 within a few minutes has been developed.

About 2-3 ml of homogeneous PEGDA 700 + 5% (w/w) HA with 0.5% (w/w) Irgacure 819 solution is sufficient to produce a 150x150 mm membrane with a layer thickness of about 200 to 300 µm. To achieve an even distribution of the hydrogel within the sandwich construction, slight movements of the glasses were made. In this way, even thinner layers could be accomplished. Furthermore, a foldback clamp maintained the required pressure to accomplish the necessary layer thickness even after curing for ten minutes in the UV chamber.

Figure 4: Explosion diagram of PEGDA + HA membrane fabrication. COC foils were taped on the glass slides to prevent the PEGDA from adhering to the glass. The PEGDA 700 with HA mixture was dripped onto the construction. Both glass slides created a sandwich construction, in which the composite was pressed to a thin layer. Afterwards, it was cured under UV for 10 minutes.

After curing, the membrane was cut out with the laser cutter with the following settings (Table 4).

	Cutting			Engraving			
	Thickness	Speed	Velocity	Frequency	Speed	Velocity	Frequency
PEGDA 250	0.1 mm	40	2	1000	20	2	1000
PEGDA 700	0.15 mm	40	2	1000	35	2	1000
Cello-phane	0.1 mm	40	2	1000	100	0.5	1000
Adhesives	0.8 mm	80	2	5000	56	100	500

Table 4: Settings of Laser Cutter (Trotec Speedy 100) for membranes and adhesive

Using the engraving parameters, we achieved holes with a diameter of 100-150 µm (Figure 5). The membranes were briefly washed in dH_20 to remove accumulated dust, which caused them to swell several millimetres and had to be considered when cutting out the membranes. The opposite effect was observed during sterilisation with EtOH and H_2O_2. As a result of moisture removal, the membranes warped and tore apart. In order to counteract these effects, the layer thickness was slightly increased to approximately 300 µm.

The holes in the membranes contribute to an adequate supply of nutrients and drives individual cells to accumulate in the openings and form small aggregates.

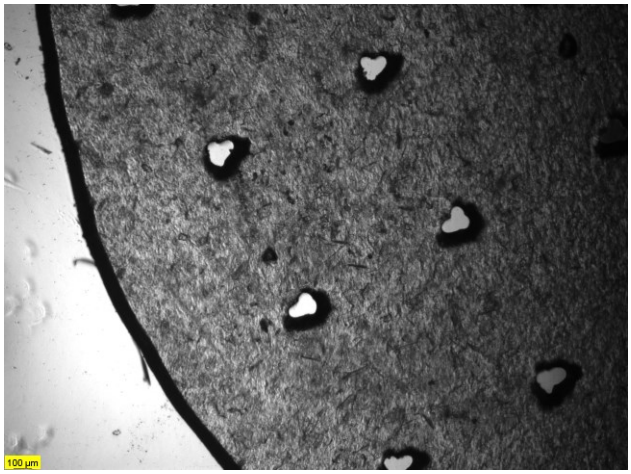

Figure 5: PEGDA 700 + HA membrane with around 100 µm holes cut by Laser Cutter (Trotec Speedy 100). Image captured on Leica S8APO Binocular Stereo Microscopy

4.4. Comparing UV Treatment and Plasma Treatment on PEGDA 700 - HA Hydrogel

In order to facilitate membrane attachment, two methods were employed as the adherence of cells to untreated PEGDA constructs was not possible. Long exposure times

under UV light and a short plasma treatment induced a conformational change in the surface of PEGDA and other materials [6, 7, 9]. Our results indicated that plasma-treated membranes exhibit stronger adhesion for cells, spheroids and extracellular matrix. A long-term experiment lasting 77 days, comparing cells on UV- and plasma-treated hydrogels, demonstrated that seeded single cells (cell concentration $3x10^5$) tend either to outgrow the membrane's surface or to form large aggregates.

After a week, small spheroids became apparent on plasma-treated and UV-treated surfaces and proliferated over several weeks. In the first 20 days, the spheroids showed cell expansions as if they were sensing the surface for possible binding sites (Figure 6 A and D). Furthermore, on both treated membranes, observations displayed that spheroids may have evolved from the cell aggregates that developed in the pits, indicated by a large quantity of smaller spheroids next to holes (Figure 6 B and F). The size of the spheroids varied extensively, when comparing both treatments. The largest spherical aggregate was discovered on day 41 (Figure 7 F) on the UV-treated hydrogel and had a size of approximately 800 µm. In comparison, big cell aggregates on plasma-treated hydrogels reached a diameter of around 450 µm (Figure 7 B and E).

Due to the vast number of unequal-sized aggregates on the UV-treated membrane, it could be observed that spheroids repeatedly detached from the membrane and were removed during medium exchange. Additionally, floating spheroids were reunited to form smaller aggregates and subsequently attached to the hydrogel again.

On both approaches, after sensing the close surrounding, the aggregates tend to fuse together and form bigger constructs (Figure 6 C and F) and either staying in a spherical formation or outgrow.

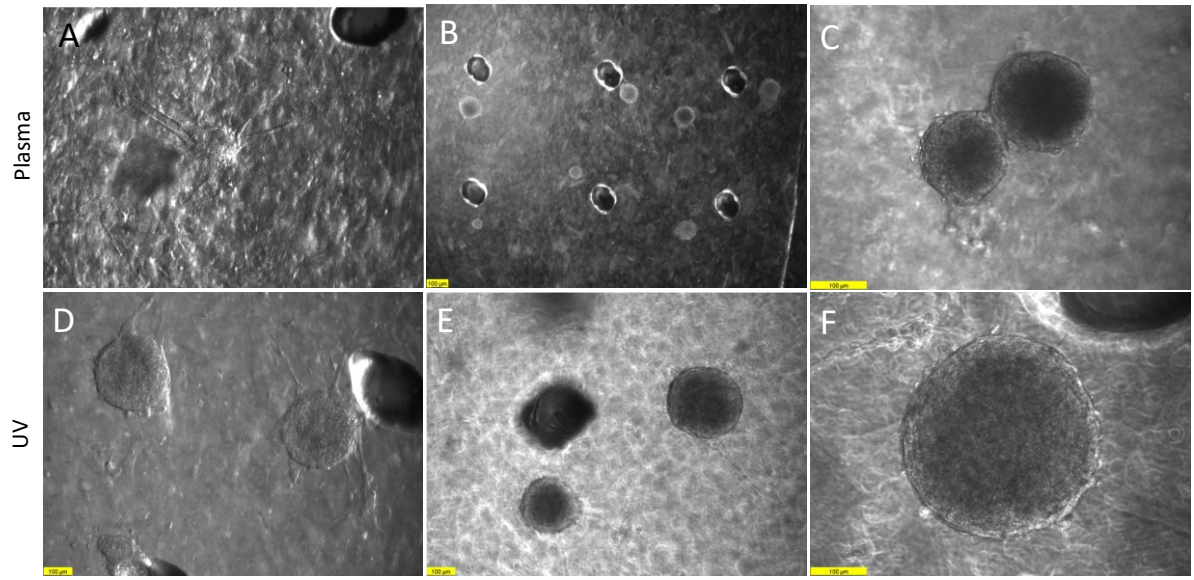

Figure 6: Human fetal osteoblast (hFOB1.19) single cells were seeded on plasma- and UV-treated PEGDA 700 + HA hydrogels (day 11-14). First, spheroids were detected on day 11 ***(A and D)****. Cell extensions could already be seen palpating for possible attachment sites.* ***(B and E):*** *Most spheroids were found around the excised holes, suggesting that the spheroids develop in the troughs and move onto the membrane (day 12 and 14****).*** ***(C and F):*** *On both hydrogels, the spheroids connect together and form themselves to large aggregates (both day 14). All images were captured on Leica DMiL using the LAS X Software (Leica).*

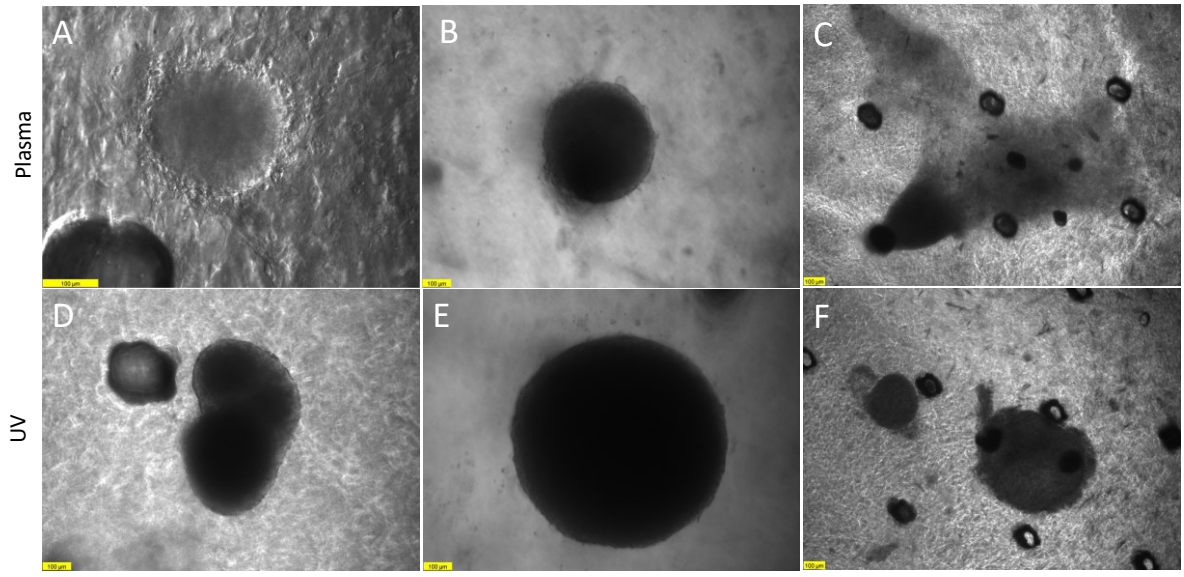

Figure 7: Human fetal osteoblast (hFOB1.19) single cells were seeded on plasma- and UV-treated PEGDA 700 + HA hydrogels (day 19-70); ***(A):*** *Spheroids form cell extensions and spread around the surface of the hydrogel (day 19).* ***(B and E):*** *The spheroids continued to form larger structures. Especially on the UV-treated membrane, a substantial enlargement could be observed, but only a low spread-out on the hydrogel (both day 41).* ***D:*** *newly formed spheroids fusing together (day 29)* ***(C and F):*** *On day 70, especially on the plasma-treated hydrogel, a considerable cell lawn spread around the surface and created different shapes and layers of cells. The structure of the UV-treated was not as tight as the*

plasma-treated membrane, indicating a lower adhesion possibility. All images were captured on Leica DMiL using the LAS X Software (Leica). The scale bars in the left corners indicate 100µm.

During both approaches, it became apparent that newly formed spheroids exhibit a tendency to explore their environment using cellular extensions, and when possible, fuse with adjacent spheroids (Figure 7 A and D).

In addition to differences in size (Figure 7 B and E), variations in the extent of cell spreading were also observable. On the plasma-treated membrane, it has been shown that cells encountered more opportunities for adhesion and consequently spread across the entire hydrogel. In contrast, on the UV-treated membrane, only individual Spheroids were capable of adhesion and comparatively spread in a limited amount.

The subsequent figure (Figure 8) illustrates of how much the cells have spread on the plasma-treated hydrogel.

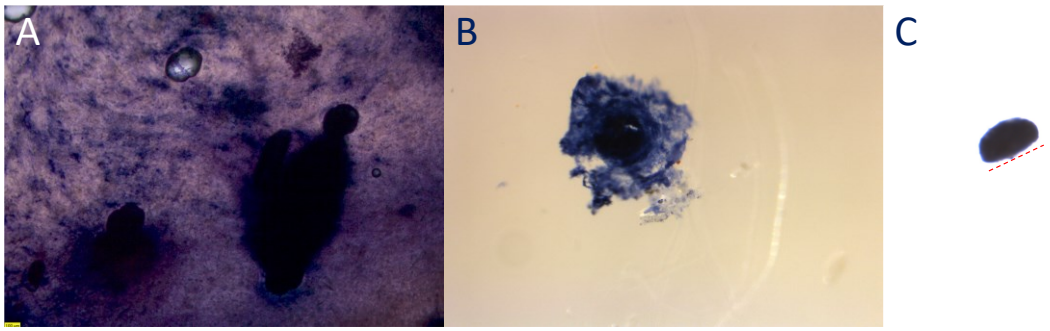

Figure 8: ALP-stained cells and spheroids formed from single hFOB cells detached from PEGDA 700 + HA hydrogel. ***(A):*** *Alkaline Phosphatase staining of the hydrogel allowed visualisation of the cells on the membrane. A spreading of the cell lawn over the entire membrane as well as large and misshapen cell aggregates could be seen. Leica DMi8 microscope and acquisition was performed with LAS X software (Leica). Images of detached spheroids with surrounded cell mass* ***(B)*** *and flat edges* ***(C),*** *captured with Leica S8APO Binocular Stereo microscopy and with Leica MC170HD. Both pictures were taken at a magnification of 6.4x.*

After 77 days, the experiment was stopped, and both membranes were stained with alkaline phosphatase. This indicated how broadly the cells spread on the membrane and how they generally behaved on a bone-like hydrogel. After fixation and staining, the cells were removed from the membrane with tweezers and analysed microscopically.

Loosening the fixed aggregates and subsequent observation with Leica S8APO Binocular Stereo microscopy made it possible to visualise that the spheroids spread all over the hydrogel and that cell masses formed around the core (Figure 8 A). The entire hydrogel was covered with a cell lawn. Darker areas represent multi-layered levels that indicate possible 3D structures. Furthermore, the spheroids tend to grow laterally over

the edges of the membrane, which resulted in an observable increase in cell mass (Figure 8 B-C).

4.5. Comparison of Spheroids in a HA and non-HA Environment

A standard method to investigate the differentiation of spheroids is fluorescence staining. Here, we were particularly interested in calcification and the expression of alkaline phosphatase [8, 24]. 5% (w/w) of the bone-like mineral was added to the PEGDA 700 with 0,5% (w/w) Irgacure 819 hydrogel to compare cell aggregates in hydroxyapatite and non-hydroxyapatite environments. Studies with similar tasks usually exceeded this amount of HA [14]. We were able to show that more hydroxyapatite led to coarser and opaque structures, and the aggregates were no longer distinguishable from artefacts.
For spheroids in the HA environment, an average of ten three-day-old spheroids were transferred onto hydrogel membranes of a 6-well plate and incubated for three days at atmospheric conditions at 34°C and 5% CO_2. This procedure provided enough time for the spheroids to bind to the membranes and proliferate. In order to avoid any loss, sufficient medium was provided, and the movement of the plate was reduced to a minimum.
On the seventh day, aggregates from one well were treated with the immunofluorescent marker xylenol orange. Spheroids were stained overnight and then cultured with a transparent DMEM medium. The control and the spheroids for ALP staining were previously fixed with PFA. Afterwards, alkaline phosphatase activity was detected with ALP dye overnight (supplementary protocol).

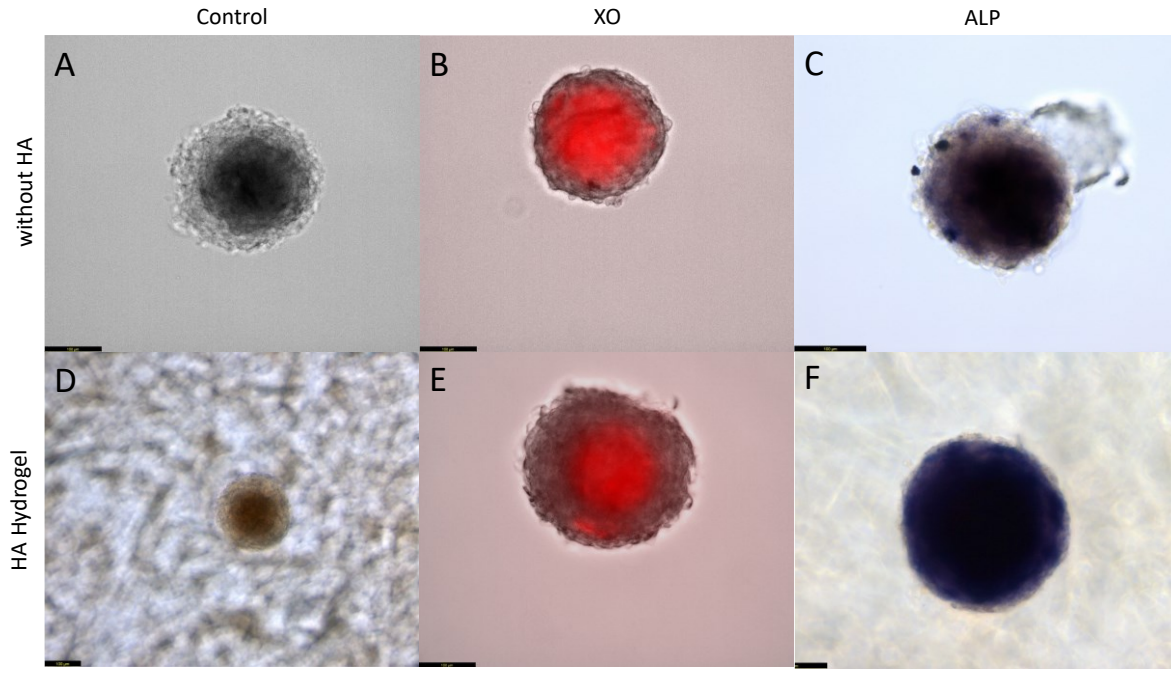

Figure 9: Staining of hFOB spheroids with XO and ALP on and off HA. ***(A-C):*** *Images of seven-day-old spheroids from a 96-well plate in a no-HA surrounding.* ***(A):*** *Control,* ***(B):*** *Xylenol Orange staining;* ***(C):*** *Alkaline Phosphatase staining;* ***(D-F):*** *Spheroids were cultivated in a 96-well plate for two days before they were placed onto a PEGDA 700 + HA hydrogel. On day seven of cultivation, the spheroids were stained with* ***(E):*** *Xylenol Orange and* ***(F):*** *Alkaline Phosphatase. All images were captured with a Leica DMi8 microscope and acquisition was performed with LAS X software (Leica). The scale bar on the left corner indicates 100µm.*

There was no noticeable difference after comparing the controls (Figure 9 A and D). In both cases, a slightly denser accumulation of cells could be identified in the core regions, and they were almost identical in size. Nevertheless, a clear difference could be seen in the XO staining. Spheroids that have not been in an HA environment had a discernibly higher calcification (Figure 9 B) compared to aggregates in HA environments (Figure 9 E). Our results demonstrated that calcium is produced almost to the very outer edges of the control spheroids. Only a few outer cell layers show little or no calcification. However, spheroids that had been cultured in an HA environment for four days, exhibited calcification mainly in the core. In the outer layers, the production of calcium was visibly reduced.

Since ALP is an essential factor in the mineralisation of bone, ALP staining was performed on seven-day-old spheroids [6, 7]. Unpublished results of the research group showed that spheroids on nano-hydroxyapatite reduce the production of alkaline phosphatase.

However, our results displayed that spheroids in a hydroxyapatite environment increase the expression of ALP. Figure 9 F shows that the production of ALP was visibly increased compared to cells in a non-HA environment. In untreated spheroids, the

expression was slightly higher in the core but decreased further into the outer layers (Figure 9 C).

The relatively large aggregates in Figure 6 F resulted from extending spheroids on plasma-treated membranes (cell outgrowth as described in 4.4). After fixation and later separation from the membrane, the aggregates were found to be flattened on the contact side and thus moved their mass outwards (Figure 8 C).

4.6. Creating Microfluidic System operated by Syringe Pump System

Microfluid systems appear in different forms in the scientific literature, depending on the application [4, 8, 16, 25]. For our approach, we developed a straightforward design that could be rapidly manufactured and consisted of only a few components. Within the microfluidic chip, a chamber with a diameter of 9 mm was designed, capable of accommodating a volume of approximately 300 µl, which appeared to be adequate for our purposes. Furthermore, the chamber provided enough space for the placement of a hydrogel membrane (Figure 10).

For this purpose, a PLA chip was 3D-printed with the aid of a Prusa thermoplastic printer device. The print was subsequently roughened with sandpaper to improve the surface finish. Furthermore, the tubes were inserted and sealed with epoxy glue. On the underside, a construct composed of double-sided adhesive tape and cellophane film was attached (Figures 10 and 11 A). This provided the necessary connection to the component. Opening the chip at start was necessary cell injections and to ensure gas exchange within the incubator. The chip was closed with a BioRad foil was used. The foil showed solid adhesive strength for easy and quick application.

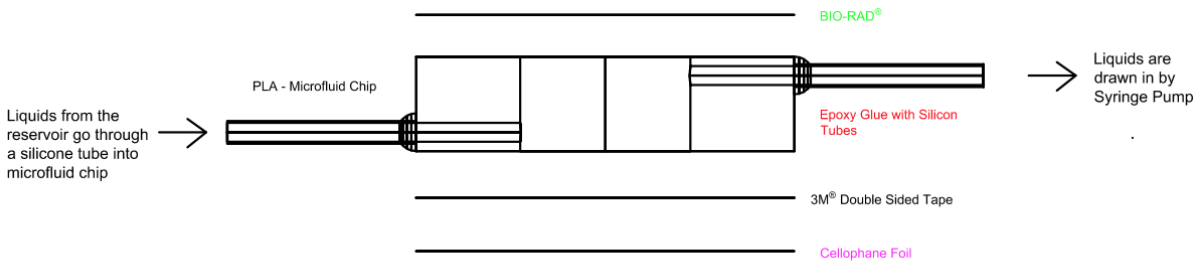

Figure 10: Schematic representation of the microfluid chip, divided into the respective layers. Two silicon tubes for the inlet and outlet were glued into the PLA print by epoxy glue. A sandwich construction of double-sided adhesive tape (3M) with cellophane was attached to the underside. A BioRad film was used to seal the top side.

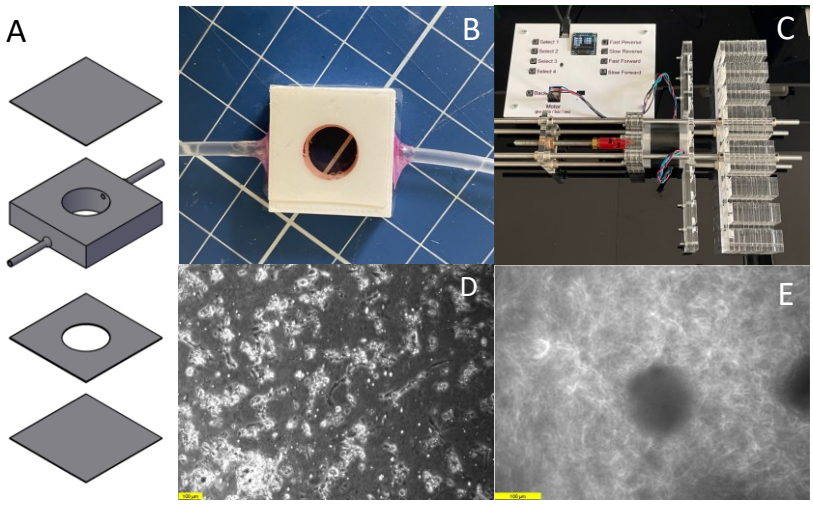

***Figure 11**: Devices for cell culture specific analyses using microfluidic chips; **(A):** 3D image of microfluidic chip; **(B):** Top view of an operating microfluid chip; **(C):** A self-designed syringe pump system comprised of a control panel and a stepper motor driven pump system. Up to seven possible syringes can be operated simultaneously. The modules for different sizes can be easily exchanged; **(D):** hFOB 1.19 single cells were seeded on cellophane and allowed to adhere for 24 hours. Sufficient oxygen and CO_2 were introduced through pierced BioRad foil to prevent suffocation. The next day, the BioRad foil was replaced, and cultivation was started using the syringe pump. The picture shows adherent cells on the cellophane after three days of cultivation as well as a lot of dust and particles; **(E):** Image of a spheroid on PEGDA 700 + HA hydrogel in a microfluidic chip. The spheroids were transferred to the membrane after two days of cultivation in a 96-well plate. After 24 hours for settling down and adhering to the substrate, the pump system was started for further cultivation. Images was taken through the membrane, and both pictures **(D and E)** were captured with Leica DMiL using the LAS X Software (Leica).*

Originally, efforts were undertaken to cultivate spheroids on hydrogels within a microfluidic chip. The cell aggregates derived from hFOB cells, with a seeding density of 10^3 cells per well, were cultured within a U-bottom plate and subsequently transferred onto the membrane after a two-day incubation period. The aggregates were cultivated within the chip for further 24 hours to ensure adequate attachment. Afterwards, the syringe pump and the automated cultivation processes were initiated.

However, only inadequate results could be achieved, primarily due to the challenge of eliminating air bubbles in the system. These bubbles became entrapped within the PEGDA hydrogel and aspiration methods showed only little effects. Furthermore, applying an external force to the chip yielded only limited success and led to the detachment of spheroids from the membranes. To obtain meaningful results, a different approach was employed. After the attachment period, the chip was inverted, as microscopic analysis through the hydrogel was inadequately informative (Figure 11 E). However, the hydrogel became wedged with the remaining air bubbles, which made it very challenging for the membrane to lie flat thus largely restraining microscopic analysis.

For the 2D cell culture approach, single cells ($2x10^4$ cells per chamber) were seeded on a cellophane base inside the device. In certain experimental approaches, the

presence of contaminants affected cell observation, attachment, and growth within the chamber (Figure 11 D). To counteract this issue in future experiments, a sterilised, unused cellophane roll within the cell culture hood should prevent dust and other particles from getting onto the foil in the first place.

Equipped with our self-designed and programmed syringe pump system, we were able to select from four pre-programmed programs with various speed settings for syringes from 1-ml up to 5-ml. Furthermore, we developed various PMMA attachments for syringes, enabling the operation of up to seven syringes simultaneously. The four pins of the stepper motor were plugged into the provided device connected to the stepper motor driver. This driver converted the 3.3V output voltage of the Teensey 4.1 microcontroller to the required 12V of the stepper motor. A Sony 19.5V power supply with 4.7A was used to operate the stepper motor driver (Figure 12 A-B).

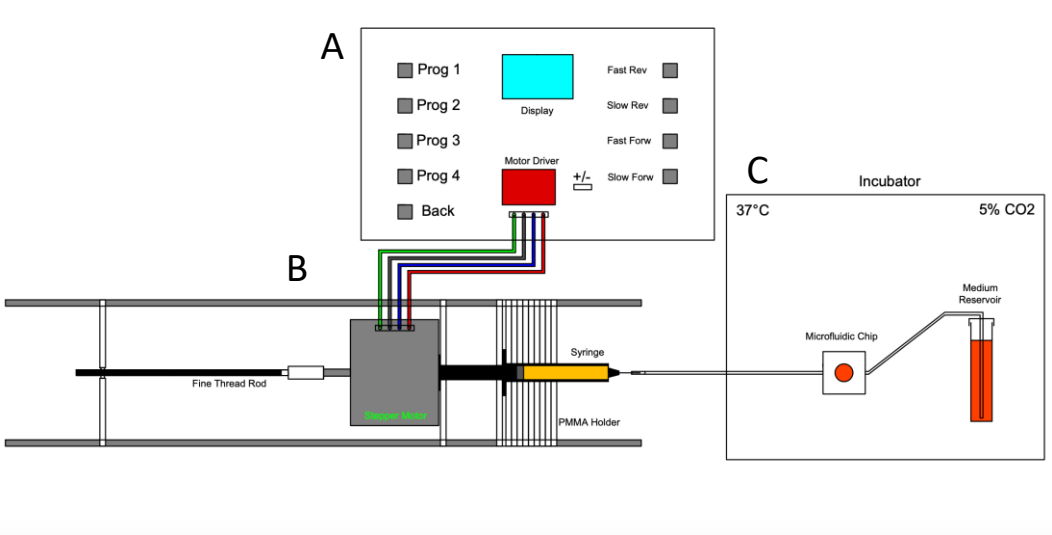

*Figure 12: Schematic representation of the experimental setup. This represents the input panel (**A**), the pump system (**B**) driven by the stepper motor and the incubator (**C**) in which the cells were cultivated.*

Additionally, the control panel featured buttons programmed for manual adjustments, offering two speed options for forward and backward motorisation. The comprehensive material list of the syringe pump, along with the Arduino code is attached as a supplementary protocol (8.2). The code was written in C++ using the freely available Arduino IDE software, facilitating straightforward code modification and adaptation to suit specific application requirements. The desired flow rate can be calculated and changed using the formula below. The formula describes the speed of the stepper motor in revolutions per minute of the respective syringe used.

$$1\mu\frac{l}{\min} \triangleq \textit{Delay Time of } 835ms \textit{ per Step}$$

For a 1-ml syringe, a delay time of 835ms to accomplish a flow rate of 1-µl per minute. The delay time indicates how long the stepper motor pauses before it takes another step. The flow rate was discovered through trial and error and can be extended to syringes up to 5-ml.

```
1   void move4() {
2     //the microcontroller counts the ms since the start = millis()
3     unsigned long start_time = millis();
4
5     // Programm counts the ms and runs until it reaches the defined time (24h = 8.6E7ms)
6     while (millis() - start_time < 8.6E7) {
7       // Pressing backButton during movement, returning back to main manu and motor stops
8       if (!digitalRead(backButton)) {
9         updateMenu();
10        return;
11      }
12      // Ansonsten wird das Programm in Endlos-Schleife wiederholt
13      digitalWrite(dirPin, HIGH);   // Forward Direction = LOW, Backward = HIGH
14      digitalWrite(stepPin, HIGH);  // Step is executed
15
16      delay(1670);                  // 1670 delay time correlates to 2,5µl/min of a 5ml-Syringe
17      digitalWrite(stepPin, LOW);   // Stops the Step
18    }
19    updateMenu();
20  }
```

Figure 13: Arduino IDE code of the stepper motor function. Row 16 describes the delay time for a 5-ml syringe, resulting in a flow rate of 2.5 µl per minute. Row 6 describes the automatic termination of the programme after 24 hours. The complete code can be found in the supplementary protocol.

Figure 13 displays the primary function within the Arduino code. In line 6, the duration (8.6E7 milliseconds equals 24 hours) for which the syringe should operate continuously is defined. In addition to the initialization of the stop button in line 8, the delay function (line 16) plays a crucial role. This function introduces a delay in milliseconds, representing the calculated flow rate.

This whole system represents a cost effective, user-friendly, and adaptable device suitable for a wide range of applications and can be used as an alternative to expensive laboratory pumps.

5. Discussion

5.1 PEGDA 700 + HA Hydrogel Membranes

The advancement of biocompatible hydrogels has developed a new field in regenerative biology. Polyethylene glycol diacrylate (PEGDA) 700, with its longer polymeric chain length, offers an ideal scaffold for cell research and tissue engineering, owing

to its highly favourable properties. Based on its elastic and supporting characteristics, simulating bone-like environments in a future orientated manner is now possible [8].
A large part of this master's thesis has been dedicated on developing hydrogels employing PEGDA. Hydrogels have evolved to a universal instrument due to their wide range of applications, especially in tissue engineering. Scaffolds fabricated from polydimethylsiloxane (PDMS) and PEGDA are frequently utilised due to their biocompatibility, easy prototyping, and inexpensiveness [3, 6, 16].
An objective of this thesis was to develop an inexpensive hydrogel to investigate 3D development and potential differential differences of osteoblasts when cultivated on bone-like inorganic mineral. We, therefore, prototyped a PEGDA 700 with hydroxyapatite (HA) membrane capable of supporting cell and spheroid cultivation. Numerous studies highlighted that with current 3D printing methods, solid structures made of PEGDA for cell culture can be assembled easily [2, 6, 7].
Printing PEGDA membranes with longer polymer chains with the aid of SLA printers is a complex process that often leads to imprecise assembly and the production time exceeds rapid prototyping [10, 11]. Our method enabled the assembly of hydrogels with higher molecular masses below 30 minutes, only by employing a glass-membrane construction. Furthermore, when working with PEGDA, an essential substance for polymerisation is the photoinitiator Irgacure 819, which is necessary yet often negatively affects cells [6]. Hence, we enhanced cytocompatibility by reducing the concentration from the photoinitiator from 1% (w/w) (manufacturer's specification) to 0.5% (w/w), which allowed to fully omit rinsing steps [7].
Initial experiments revealed that cells and spheroids attach, grow, and partially overgrow the membrane after plasma or UV treatment had been carried out. Interestingly, it could be demonstrated that cells attach to the plasma-treated membrane more effectively compared to those treated with UV alone. Furthermore, cells cultured on UV-treated membranes tend to form larger spheroids, suggesting a reduced availability of attachment sites.
These pre-treatments were essential to ensure the overall adhesion of cells on the membranes. Similar outcomes have been reported in other studies, indicating that these pre-treatments are necessary [6, 7].
These initial investigations demonstrated the suitability of these hydrogel membranes for conducting 3D cell culture experiments. we were able to show that spheroids and even large cell complexes, some with unusual shapes, could thus be formed. Warr et

al. discovered similar deformed 3D structures when seeding fibroblast cells onto low-adherence PEGDA 258 devices [7]. Both results indicated that the cells converge to form a 3D mass to find possibly more adherent structures on the PEGDA surface.
Additionally, PEGDA 700 HA hydrogels offer an ideal framework for cell research due to their higher polymeric chain length, resulting in increased elasticity [8], mechanical strength, porose network structure [14], and the easy uptake and discharge of substances like growth and differentiation factors [10]. Growth factors such as Exendin4 [10], TGF-beta or BMP [26] have the potential to stimulate mineralisation by continuously releasing factors stored within the membrane. Furthermore, pathways like Wnt, BMP2 or FGF are responsible for alkaline phosphatase (ALP) production and could accelerate bone formation in our system [19].
These characteristics, as well as the cost-efficient and straightforward fabrication, indicate a promising approach for organ-on-a-chip applications observing the differentiation of stem cells in hard-tissue environments.

In addressing one of the research questions, we have demonstrated that the expression patterns of cells on hard-tissue membranes differ from cells in ordinary tissue culture (TC) dishes.
Our experiments showed that cells on hydroxyapatite hydrogels produced less calcium but more alkaline phosphatase. This reduction in calcium may be explained by the fact that cells that already sense calcium in their environment need to deposit and enrich Calcium to a lower extent. Another possible hypothesis could be that the cells already reside on or next to hard tissue and thus no longer need to produce Ca^{2+} in high amounts. However, a huge amount of Ca^{2+} is needed for the mineralisation process, and many calcium-binding proteins are necessary to bring especially ALP to the cell surface [19].
Our results and those of other research groups have shown that osteogenic stem cells spread and proliferate on HA in combination with hydrogels [14, 16]. However, unpublished results from our workgroup have shown that cells binding particulate hydroxyapatite reduce the expression of ALP, which contrasts with these results. Additional publications have reported that cells on nano HA increase the expression of ALP [16, 18]. Liang et al. showed that ALP is elevated, but the expression is significantly reduced at a nano-hydroxyapatite concentration of 50 µg/ml compared to 25 µg/ml [18]. In our experiments, we worked with more than ten times the amount and did not involve

nano HA. Consequently, the result can only be compared with to published data to a limited extent.

However, according to the literature, increased ALP expression indicates mineralisation and further bone formation [19, 27]. Additional experiments would still have to be carried out. In particular, expression patterns of ALP, osteocalcin and osteopontin would be interesting, providing information on calcification, differentiation [16, 18], mineralised extracellular matrix, and early bone formation [28]. Additionally, a meaningful control could not be established as our attempts to culture osteoblast cells on pure PEGDA 700 were unsuccessful. Despite the limitations, a visible increase in ALP was observed during an experiment, which led to mineralisation. However, this study could not definitively confirm the possible development of mineralised extracellular matrix or the formation of differentiated structures.

5.2 Novel Cytocompatible Materials for Cell Culture Applications

While developing and prototyping, we encountered new materials with the potential to play an essential role in the innovation of future microfluidic systems. Furthermore, we discarded materials that were surprisingly toxic to the highly sensitive human fetal osteoblast (hFOB) 1.19 cell line, even though these materials were frequently used in the literature [3, 20]. We have demonstrated that commonly used household products such as cellophane or epoxy glue possess favourable attributes for cell culture applications and can be used without concern.

Polymethylmethacrylate (PMMA) and Polytetrafluorethylene (Teflon), often used in developing microfluidic devices, performed poorly during cytocompatibility tests. Potential reasons for this outcome could be associated with the composition of the materials. In the case of Teflon, fibres and crumbs were released after processing, which may had an impact on cellular behaviour. However, the exact reasons were unknown.

After eliminating PMMA and Teflon, the material Polylactic Acid (PLA) proved favorable for manufacturing microfluidic devices. PLA is one of the most widely utilized thermoplastics in 3D printing, characterised by its excellent properties for prototyping due to its high biocompatibility, availability, low autofluorescence and cost-effectiveness [3]. PLA proved to be a successful filament for 3D printing by using standard 3D printers like Prusa technology, with a layer thickness ranging from 100 to 150 µm. Moreover, the material exhibits high moulding and laser-cutting properties and can be considered as an alternative to PDMS [3]. Compared to stereolithography (SLA), filament-

based 3D printing performs better regarding time-efficiency, cost-effective material usage, and post-processing.

Microfluidic chips could be prototyped of Cycloolefin Copolymer (COC) filament. Printing designs on foils such as cellophane or COC leakage-free was possible but not as precise as with PLA. However, the resolution limit was reached for structures smaller than 1-mm. Hence, switching to manual drilling or SLA printers became necessary, depending on the specific application requirements.

In addition to PLA, cellulose hydrate, commonly known as cellophane, is a cheap and versatile material. Cellophane is a recyclable material and thus provide a firm basis as a material for switching from plastic to compostable and biodegradable cell culture utensils. An essential aim in the near future is to create degradable cell culture disposables to counteract the extensive plastic waste in laboratories. In preliminary investigations, we tried to develop a scaffold for cell culture based on natural products, with cellophane as the basic substrate. Yet, natural untreated products such as wood (spruce) or bones (deer) proved unsuitable.

By coating the wood with materials such as printer's wax or liquid epoxy, we achieved initial success in terms of biocompatibility, but at the cost of biodegradability. Therefore, further research should be directed towards this aspect.

One of the most notable advantages of cellophane is that plasma treatment unfolds cellulose adhesive properties comparable to tissue culture (TC) dishes. In addition to its cost-effectiveness, biocompatibility, ecological, and adhesive properties, it has been demonstrated that the cellophane foils can also be molded into various shapes [25]. Initial experiments have revealed that steep flanks in an accordion manner and small bowls were pressed with conventional screw clamps and that cellophane retains its shape over an extended period.

The research group of John Dunlop studied the geometry of different shapes that stimulated cells to proliferate and develop 3D structures. Their findings revealed that cells accumulate and proliferate faster at sharp edges than on a straight surface. Furthermore, they demonstrated that the curvature of the structure influences the expansion of 3D structures. [23].

We tried to reproduce this in our experiment applying cellophane. hFOB cells were placed on the folded plasma-treated cellophane foil to observe potential 3D formation. These cells were cultured for 43 days and monitored microscopically owing to the excellent transparency of cellophane foil.

During the first days, cells appeared to spread parallel to the flanks in the groove. Some spheroids were already observed after only a few days, but only around the channels. Over time, when the membrane was fully confluent, the spheroids increased and gained in size and eventually migrated towards the groove. However, the curvature-driven growth, as described in *Rumpler et al.* [23] was not visibly detectable. The steep flanks limited the areas that could be effectively visualised at any given time. The accumulating cell debris and the growing cell lawn made microscopic operations challenging. A new experimental approach would ease these problems. A possible solution to approach this issue might be to position the angled foil in an aperture that can be rotated. This could make microscopic procedures easier.

Other research groups have also endeavoured to construct microfluid systems utilising cellophane [25]. However, their approach involved utilising polyvinyl chloride (PVC)-coated cellophane, which was formed and sealed under high-pressure heat conditions. In contrast, uncoated cellophane has a significant disadvantage as it does not bond with other cellophane substrates.

We counteracted this challenge with sealants such as epoxy, FixoGum or double-sided tape to address this challenge. However, manual manufacturing or laser cutting was too vague to bond precise structures such as channels. Both epoxy glue and FixoGum are suitable adhesives for possible use in microfluid system development. Epoxy glue, in particular, is well-established in the industry in a wide range of applications and has been used for a long time. Additionally, the double-sided tape by 3M™ also demonstrated strong adhesion and excellent biocompatibility properties, primarily used for sealing bases, layers and membranes.

During prototyping, a problem arose concerning the curing time and the characteristics of the surfaces. Especially with PLA prints, the smooth surface was roughened with sandpaper to achieve a permanent seal.

Sterilisation and subsequent conditioning was considered essential during our materials analysis. The working group successfully established an easy method to sterilise and subsequently condition materials for at least 24 hours [6]. This step facilitated the utilisation of materials initially assumed as toxic, which thereafter could be used successfully for applications in cell culture.

5.3 Prototyping Organ-on-Chip Microfluidic Systems

Based on these innovative results described above, the goal was to develop a microfluid system to carry out standard laboratory experiments and cultivate cells and

spheroids on hydrogels over several days. In addition to the continuous medium exchange facilitated by the herein described development of a syringe pump, an important consideration was the possibility of optical visualisation using a microscope.
Subsequently, it became evident that PDMS was not promising for fast and cost-effective prototyping, and its properties proved to be suboptimal for our requirements. PDMS is one of the most frequently used materials in the scientific literature for developing microfluidic systems [2, 6, 16, 21]. Due to well established methods and enabling methods such as plasma bonding or microstructure embedding, yet also specific material properties such gas permeability, it is often utilised in organ-on-chip applications [21].
Fast and cost-effective prototyping was a substantial requirement in this thesis, promoting alternative materials with promising attributes for microfluidic systems. Especially the aspect of easy reproduction of such systems had a noteworthy influence on our decision.
As described above, the primarily used materials for the fabrication of these systems were the thermoplastics PLA and COC. Using these cost-effective thermoplastics and the wide accessibility of 3D printers has now enabled the possibility to go for industrial scale and fast prototyping simultaneously [3, 21].
After the post-printing procedures, we employed the established method for sterilisation, conditioning and cultivation [2]. This protocol appeared sufficient to ensure the successful adhesion of cells on the membranes and avoid contaminations. Following the seeding of cells or spheroids onto the membrane, an adhesive tape inhibited the cells from drying out, while a minor puncture in the foil prevented the cells from suffocating, thus allowing them to adhere. The BioRad foil was removed after 24 hours of cultivation and replaced with a new one before the actual cultivation was started with the aid of the pump system.

Throughout cultivating, it has been shown that the high humidity in the incubator greatly influenced the adhesives of our system. The curing time of the epoxy glues was not maintained at the beginning, and the smooth surfaces of the PLA prints resulted in numerous leaking trials. The biggest challenge encountered in this thesis was the persistent presence of air bubbles in the systems, which prevented the realisation of one of the primary goals. Despite multiple trials and efforts, bubble formation could not be prevented by aspiration, which resulted in the loss of cells or spheroids. In addition to

the visual restriction of bubbles in the system, built-in membranes did not yield the expected outcomes, resulting in the development of microfluidic systems without integrated membranes or hydrogels.

Eliminating air bubbles in microfluid systems is an increasingly covered topic in the scientific literature. Components such as trapping or venting are often integrated into chips, enabling a bubble-free system [20]. Zaho et al. have developed a novel and promising system in this regard. They constructed hydrophilic channel openings with a superhydrophobic surface on the outside. Due to the small distance between the two treated channels, a non-leaking liquid column can be formed, which makes it possible to filter out any air bubbles in the system [20].

This complex but seemingly effective method could bring forth the necessary results in our system thus permitting to perform cell culture-specific experiments bubble-free. This method would certainly be an asset, especially concerning a circulatory system driven by a self-developed pump system. The low oxygen permeability is another consideration in thermoplastic microfluid systems [3]. Ongaro et al. and our findings have shown that cells in a closed system tend to die after only a few hours [3]. Consequently, the establishment of a system in which O_2 and CO_2 enriched medium constantly supplies the cells is essential for long-term cultivation.

To address this need, we developed a straightforward and cost-effective programmable pump system operated by a microcontroller. Conventional pump systems, primarily used for microfluidic applications, are often bulky and very expensive. Here, reproducibility, easy handling and a cost-effective alternative to expensive laboratory equipment played a future-oriented role in our decision.

Utilising our self-developed pump system, we were able to precisely configure the necessary flow rate to achieve a complete exchange within 24 hours, thus ensuring constant cultivation for over two days. Our system was designed to utilise syringes from 1-ml up to 5-ml. However, a limiting factor was the low volume of the syringes and the flow rate. Employing syringes above 5-ml would flush out cells and spheroids from the microfluidic chamber due to the prevailing forces. Additional experiments would need to be carried out to determine whether the flow rate could be further reduced, resulting in the extension of the cultivation period.

Due to the difficulty of eliminating air bubbles within the microfluidic chip, the concept of an integrated hydrogel within the chip was abandoned. Instead, an attempt was made to establish a 2D-cell culture approach on cellophane substrate within the chip.

The favourable cell-specific properties enabled an experiment, where single cells were injected into the chip and proliferation on the cellophane foil was attempted.
However, no meaningful outcome could be obtained due to the presence of contaminants that had accumulated on the foil, preventing the growth and proliferation of the cells. Cultivation utilising the self-developed syringe pump was carried out over three days, but only isolated cells were observable. To obtain valuable results, further experiments had to be carried out in a consistent manner and the contaminants need to be reduced to a minimum.
Nonetheless, these initial experiments highlight that the development and discovery of these innovations headed into the right direction. These accomplishments represent significant progress in the field of microfluidic systems development.

Conclusion

Hydrogels and microfluidic systems are increasingly employed in cell-specific procedures, benefitting from the continuous advancement in additive manufacturing techniques, thereby enabling the creation of even more complex structures. Given the widespread availability of affordable printers, resins, and filaments, a rapid and fruitful progress in this field is anticipated. Notably, simplicity, rapid production, and cost-effectiveness are key factors ensuring the facilitation of prototyping and this advancement.

In this master's thesis, it could be demonstrated that low-cost hydrogels can be easily manufactured from polyethylene glycol diacrylate (PEGDA) and can be successfully applied to perform cell culture experiments to characterize osteogenic development. These hydrogels can be altered to suit various cellular analytical applications as needed.

Materials suitable for constructing microfluid systems have been explored, including substances that may present a sustainable alternative to fossil-based products in cell culture. The deployment of plasma-treated cellophane has the potential to set new standards in 2D cell culture and could potentially replace polystyrene in the future.

Based on these findings, a microfluid system could be developed, enabling conventional 2D cell culture over multiple days. A self-designed pumping system continuously supplied the necessary nutrients to the system, and the transparency of the cellophane allowed microscopic monitoring. However, unidentified factors hindered proliferation, calling for further trials including error analysis and future adjustments. This compilation of materials, methods, and techniques could become an essential instrument in research, as they cover a wide range of applications and may simulate in vivo-like environments.

6. References

1. Li, X.J., et al., *Microfluidic 3D cell culture: potential application for tissue-based bioassays.* Bioanalysis, 2012. **4**(12): p. 1509-25.
2. Lutsch, E., et al., *A Poly-(ethylene glycol)-diacrylate 3D-Printed Micro-Bioreactor for Direct Cell Biological Implant-Testing on the Developing Chicken Chorioallantois Membrane.* Micromachines (Basel), 2022. **13**(8).
3. Ongaro, A.E., et al., *Polylactic is a Sustainable, Low Absorption, Low Autofluorescence Alternative to Other Plastics for Microfluidic and Organ-on-Chip Applications.* Anal Chem, 2020. **92**(9): p. 6693-6701.
4. Inamdar, N.K. and J.T. Borenstein, *Microfluidic cell culture models for tissue engineering.* Curr Opin Biotechnol, 2011. **22**(5): p. 681-9.
5. Salmi, M., *Additive Manufacturing Processes in Medical Applications.* Materials (Basel), 2021. **14**(1).
6. Urrios, A., et al., *3D-printing of transparent bio-microfluidic devices in PEG-DA.* Lab Chip, 2016. **16**(12): p. 2287-94.
7. Warr, C., et al., *Biocompatible PEGDA Resin for 3D Printing.* ACS Appl Bio Mater, 2020. **3**(4): p. 2239-2244.
8. Struber, A., et al., *Low-Cost Devices for Three-Dimensional Cell Aggregation, Real-Time Monitoring Microscopy, Microfluidic Immunostaining, and Deconvolution Analysis.* Bioengineering (Basel), 2022. **9**(2).
9. Scislowska-Czarnecka, A., et al., *Oxygen plasma surface modification augments poly(L-lactide-co-glycolide) cytocompatibility toward osteoblasts and minimizes immune activation of macrophages.* J Biomed Mater Res A, 2015. **103**(12): p. 3965-77.
10. Liu, W., et al., *PEGDA/HA mineralized hydrogel loaded with Exendin4 promotes bone regeneration in rat models with bone defects by inducing osteogenesis.* J Biomater Appl, 2021. **35**(10): p. 1337-1346.
11. Magalhães, L.S.S.M., et al., *Nanocomposite Hydrogel Produced from PEGDA and Laponite for Bone Regeneration.* J Funct Biomater, 2022. **13**(2).
12. Nguyen, K.T. and J.L. West, *Photopolymerizable hydrogels for tissue engineering applications.* Biomaterials, 2002. **23**(22): p. 4307-14.
13. Koski, C., A.A. Vu, and S. Bose, *Effects of chitosan-loaded hydroxyapatite on osteoblasts and osteosarcoma for chemopreventative applications.* Mater Sci Eng C Mater Biol Appl, 2020. **115**: p. 111041.
14. Wang, Y., et al., *A GelMA-PEGDA-nHA Composite Hydrogel for Bone Tissue Engineering.* Materials (Basel), 2020. **13**(17).
15. Ramesh, N., S.C. Moratti, and G.J. Dias, *Hydroxyapatite-polymer biocomposites for bone regeneration: A review of current trends.* J Biomed Mater Res B Appl Biomater, 2018. **106**(5): p. 2046-2057.
16. Tang, Q., et al., *Fabrication of a hydroxyapatite-PDMS microfluidic chip for bone-related cell culture and drug screening.* Bioact Mater, 2021. **6**(1): p. 169-178.
17. Abdul Halim, N.A., M.Z. Hussein, and M.K. Kandar, *Nanomaterials-Upconverted Hydroxyapatite for Bone Tissue Engineering and a Platform for Drug Delivery.* Int J Nanomedicine, 2021. **16**: p. 6477-6496.
18. Liang, W., et al., *Hydroxyapatite Nanoparticles Facilitate Osteoblast Differentiation and Bone Formation Within Sagittal Suture During Expansion in Rats.* Drug Des Devel Ther, 2021. **15**: p. 905-917.

19. Vimalraj, S., *Alkaline phosphatase: Structure, expression and its function in bone mineralization.* Gene, 2020. **754**: p. 144855.
20. Zhao, X., et al., *Air bubble removal: Wettability contrast enabled microfluidic interconnects.* Sens Actuators B Chem, 2022. **361**.
21. Schneider, S., et al., *Membrane integration into PDMS-free microfluidic platforms for organ-on-chip and analytical chemistry applications.* Lab Chip, 2021. **21**(10): p. 1866-1885.
22. Matellan, C. and A.E. Del Río Hernández, *Cost-effective rapid prototyping and assembly of poly(methyl methacrylate) microfluidic devices.* Sci Rep, 2018. **8**(1): p. 6971.
23. Rumpler, M., et al., *The effect of geometry on three-dimensional tissue growth.* J R Soc Interface, 2008. **5**(27): p. 1173-80.
24. Marozin, S., et al., *Kinship of conditionally immortalized cells derived from fetal bone to human bone-derived mesenchymal stroma cells.* Sci Rep, 2021. **11**(1): p. 10933.
25. Hamedi, M.M., et al., *Coated and uncoated cellophane as materials for microplates and open-channel microfluidics devices.* Lab Chip, 2016. **16**(20): p. 3885-3897.
26. Chen, G., C. Deng, and Y.P. Li, *TGF-β and BMP signaling in osteoblast differentiation and bone formation.* Int J Biol Sci, 2012. **8**(2): p. 272-88.
27. Murshed, M., *Mechanism of Bone Mineralization.* Cold Spring Harb Perspect Med, 2018. **8**(12).
28. Bailey, S., et al., *Osteocalcin and osteopontin influence bone morphology and mechanical properties.* Ann N Y Acad Sci, 2017. **1409**(1): p. 79-84.

7. Appendix

8. Supplementary Protocol

8.1 List of Abbreviations

AM	Additive Manufacturing
LOC	Lab-On-Chip
PEGDA	Polyetylene glycole diacrylate
HA	Hydroxyapatite
PDMS	Polydimethylsiloxane
PMMA	Polymethyl methacrylate
COC	Cycloolefin copolymer
PS	Polystyrene
PLA	Polylactide
Cellophane	Cellulose hydrate
Teflon	Polytetrafuorethylene
hFOB	human fetal osteoblast
HET-CAM	hen's egg test chorioallantoic membrane
ALP	Alkaline Phosphate
ALB	Alkaline Phosphate Buffer
NBT/BCIP	Nitro blue tetrazolium/ 5-bromo-4-chloro-3-indolyl-phosphate
Pi	inorganic phosphate
PPi	inorganic pyrophosphate
XO	Xylenol Orange
Wnt	Wingless Int-1
BMP2	Bone Morphogenetic Protein 2
FGF	Fibroblast Growth Factor
TGF-beta	Ttransforming Growth Factor beta
DMEM/F12	Dulbecco's Modified Eagle Medium/Nutrient Mixture F-12
PBS	Phosphate Buffer Saline
EDTA	Ethylenediaminetetraacetic acid
EtOH	Ethanol
PFA	Parafomraldehyde
SLA	Stereolithography
MW	Molecular Weigth
CAD	Computer-Aided Design

8.2 Arduino Code

```
// Library für OLED importieren
#include <Wire.h>  // Bibliothek für den I2C-Bus
#include <Adafruit_SSD1306.h>  // Bibliothek für das OLED Display
#include <Stepper.h> // Library für den Steppermotor importiern

#define OLED_RESET 4  // Reset-Pin des OLED Displays
Adafruit_SSD1306 display(OLED_RESET);  // OLED Display initialisieren

// PIN-Anschlüsse des Steppermotors definieren
const int dirPin = 31;
```

```
19  const int stepPin = 32;
20
21  // PIN-Anschlüsse der Select Buttons und des Back Buttons definieren
22  int selectButton1 = 1;
23  int selectButton2 = 2;
24  int selectButton3 = 3;
25  int selectButton4 = 4;
26  int backButton = 5;
27
28  // Die Befehle fastforward, slowforward, fastreverse, slowreverse sollen mittels Tastendruck ausgelöst wer-
    den.
29  // Der Motor soll sich nur bei gedrückter Taste bewegen.
30  int fastreverseButton = 23;
31  int slowreverseButton = 22;
32  int fastforwardButton = 15;
33  int slowforwardButton = 14;
34
35  void setup() {
36  // PINs für Motor definieren
37    pinMode(stepPin, OUTPUT);
38    pinMode(dirPin, OUTPUT);
39
40  Serial.begin(9600);
41    // I2C-Bus initialisieren
42    Wire.begin();
43
44    // OLED Display initialisieren und einschalten
45    display.begin(SSD1306_SWITCHCAPVCC, 0x3C);  // I2C-Adresse des Displays
46    display.display();
47    delay(2000);
48
49  // Buttons als Input_Pullup definieren
50    pinMode(selectButton1, INPUT_PULLUP);
51    pinMode(selectButton2, INPUT_PULLUP);
52    pinMode(selectButton3, INPUT_PULLUP);
53    pinMode(selectButton4, INPUT_PULLUP);
54    pinMode(backButton, INPUT_PULLUP);
55
56    pinMode(fastforwardButton, INPUT_PULLUP);
57    pinMode(slowforwardButton, INPUT_PULLUP);
58    pinMode(fastreverseButton, INPUT_PULLUP);
59    pinMode(slowreverseButton, INPUT_PULLUP);
60
61  // Zu Beginn soll am Display das Hauptmenü erscheinen
62    updateMenu();
63  }
64  void loop() {
65
66  //Wird der SelectButton1 kurz gedrückt, soll am Display "R U N N I N G  1" stehen sowie in der 2. Zeile die
    Flussrate.
67    if(!digitalRead(selectButton1)){
68    executeRunning1();
```

```
69    move1();
70    }
71
72   //Wird der SelectButton2 kurz gedrückt, soll am Display "R U N N I N G  2" stehen sowie in der 2. Zeile die
     Flussrate.
73    if(!digitalRead(selectButton2)){
74    executeRunning2();
75    move2();
76    }
77
78   //Wird der SelectButton3 kurz gedrückt, soll am Display "R U N N I N G  3" stehen sowie in der 2. Zeile die
     Flussrate.
79    if(!digitalRead(selectButton3)){
80    executeRunning3();
81    move3();
82    }
83
84   //Wird der SelectButton4 kurz gedrückt, soll am Display "P R O G R A M" stehen sowie in der 2. Zeile die
     Flussrate.
85    if(!digitalRead(selectButton4)){
86    executeRunning4();
87    move4();
88    }
89
90   // backButton soll immer wieder zum Hauptmenu führen
91    if(!digitalRead(backButton)){
92    updateMenu();
93    }
94   ////////////////////////
95   //MOTOR MANUELL VOR und ZURÜCK BEWEGEN
96
97   // MANUELL FAST REVERSE
98   // Lese den Wert des Buttons
99    int buttonStatefastreverse = digitalRead(fastreverseButton);
100 // Wenn der Button gedrückt wurde, bewege den Steppermotor
101  if (buttonStatefastreverse == LOW) {
102    digitalWrite(dirPin, HIGH);  // Setze die Richtung auf Vorwärts
103    digitalWrite(stepPin, HIGH); // Gebe einen Schritt aus
104    delay(2);                    // Warte 2 Millisekunden
105    digitalWrite(stepPin, LOW);  // Stoppe den Schritt
106  }
107
108 // MANUELL SLOW REVERSE
109 // Lese den Wert des Buttons
110  int buttonStateslowreverse = digitalRead(slowreverseButton);
111 // Wenn der Button gedrückt wurde, bewege den Steppermotor
112  if (buttonStateslowreverse == LOW) {
113    digitalWrite(dirPin, HIGH);  // Setze die Richtung auf Vorwärts
114    digitalWrite(stepPin, HIGH); // Gebe einen Schritt aus
115    delay(40);                   // Warte 40 Millisekunden
116    digitalWrite(stepPin, LOW);  // Stoppe den Schritt
117  }
```

```
118
119 // MANUELL FAST FORWARD
120 // Lese den Wert des Buttons
121   int buttonStatefastforward = digitalRead(fastforwardButton);
122 // Wenn der Button gedrückt wurde, bewege den Steppermotor
123   if (buttonStatefastforward == LOW) {
124     digitalWrite(dirPin, LOW);  // Setze die Richtung auf Vorwärts
125     digitalWrite(stepPin, HIGH); // Gebe einen Schritt aus
126     delay(2);                   // Warte 2 Millisekunden
127     digitalWrite(stepPin, LOW);  // Stoppe den Schritt
128   }
129
130 // MANUELL SLOW FORWARD
131 // Lese den Wert des Buttons
132   int buttonStateslowforward = digitalRead(slowforwardButton);
133 // Wenn der Button gedrückt wurde, bewege den Steppermotor
134   if (buttonStateslowforward == LOW) {
135     digitalWrite(dirPin, LOW);  // Setze die Richtung auf Vorwärts
136     digitalWrite(stepPin, HIGH); // Gebe einen Schritt aus
137     delay(40);                   // Warte 40 Millisekunden
138     digitalWrite(stepPin, LOW);  // Stoppe den Schritt
139   }
140 }
141 void updateMenu(){
142   display.clearDisplay();
143   display.setTextSize(1);
144   display.setTextColor(WHITE);
145   display.setCursor(0,0);
146   display.println("Flow rate   1 ul/min");
147   display.setCursor(0,8);
148   display.println("Flow rate   2 ul/min");
149   display.setCursor(0,16);
150   display.println("Flow rate   5 ul/min");
151   display.setCursor(0,24);
152   display.println("Program");
153   display.display();
154 }
155 void executeRunning1(){
156   display.clearDisplay();
157   display.setTextSize(1);
158   display.setTextColor(WHITE);
159   display.setCursor(0,0);
160   display.println("R U N N I N G  1");
161   display.setCursor(0,8);
162   display.println("   1 ul/min");
163   display.setCursor(0,16);
164   display.println("  60 ul/h");
165   display.setCursor(0,24);
166   display.println("1440 ul/d");
167   display.display();
168   }
169
```

```
170 void executeRunning2(){
171   display.clearDisplay();
172   display.setTextSize(1);
173   display.setTextColor(WHITE);
174   display.setCursor(0,0);
175   display.println("R U N N I N G  2");
176   display.setCursor(0,8);
177   display.println("   2 ul/min");
178   display.setCursor(0,16);
179   display.println(" 120 ul/h");
180   display.setCursor(0,24);
181   display.println("2880 ul/d");
182   display.display();
183 }
184
185 void executeRunning3(){
186   display.clearDisplay();
187   display.setTextSize(1);
188   display.setTextColor(WHITE);
189   display.setCursor(0,0);
190   display.println("R U N N I N G  3");
191   display.setCursor(0,8);
192   display.println("   5 ul/min");
193   display.setCursor(0,16);
194   display.println(" 300 ul/h");
195   display.setCursor(0,24);
196   display.println("7200 ul/d");
197   display.display();
198 }
199
200 void executeRunning4(){
201   display.clearDisplay();
202   display.setTextSize(1);
203   display.setTextColor(WHITE);
204   display.setCursor(0,0);
205   display.println("R U N N I N G");
206   display.setCursor(0,8);
207   display.println("P R O G R A M");
208   display.setCursor(0,16);
209   display.println("3,6 ml/day for 24h");
210   //display.setCursor(0,24);
211   //display.println("Pause 1h");
212   display.display();
213 }
214 // Flowrate 1: Funktion für Steppermotor-Bewegung
215 void move1() {
216   while (true){
217     if(!digitalRead(backButton)){
218       updateMenu();
219       break;
220     }
221     digitalWrite(dirPin, HIGH);  // Setze die Richtung Vorwärts = LOW, Rückwärts = HIGH
```

```
222     digitalWrite(stepPin, HIGH); // Gebe einen Schritt aus
223     delay(3340);                 // Warte 100 Millisekunden 1µl/min = delaytime 835 bei 1ml Spritze
    XXXXXXXXXXXXXXXXXXXXXXXXXXXXXXXXXXXXXXXXXXXXXXXXXXXXXXXXXXXXXXXXXXXXXXX
224     digitalWrite(stepPin, LOW);  // Stoppe den Schritt
225   }
226 }
227
228 // Flowrate 2: Funktion für Steppermotor-Bewegung
229 void move2() {
230   while (true){
231     if(!digitalRead(backButton)){
232       updateMenu();
233       break;
234     }
235     digitalWrite(dirPin, HIGH);  // Setze die Richtung Vorwärts = LOW, Rückwärts = HIGH
236     digitalWrite(stepPin, HIGH); // Gebe einen Schritt aus
237     delay(417);                  // Warte 1000 Millisekunden
238     digitalWrite(stepPin, LOW);  // Stoppe den Schritt
239   }
240 }
241
242 // Flowrate 3: Funktion für Steppermotor-Bewegung
243 void move3() {
244   while (true){
245     if(!digitalRead(backButton)){
246       updateMenu();
247       break;
248     }
249     digitalWrite(dirPin, LOW);  // Setze die Richtung Vorwärts = LOW, Rückwärts = HIGH
250     digitalWrite(stepPin, HIGH); // Gebe einen Schritt aus
251     delay(167);                  // Warte 5000 Millisekunden
252     digitalWrite(stepPin, LOW);  // Stoppe den Schritt
253   }
254 }
255 // Programm
256 void move4() {
257   unsigned long start_time = millis();
258   // start_time = Zeit in der der Motor läuft. Hier 24h
259   while (millis() - start_time < 8.6E7) {
260     // Wenn der backButton während der Motorbewegung gedrückt wird, kommt man zurück ins Hauptmenü
    und der Motor stoppt.
261     if (!digitalRead(backButton)) {
262       updateMenu();
263       return;
264     }
265     // Ansonsten wird das Programm in Endlos-Schleife wiederholt
266     digitalWrite(dirPin, HIGH);   // Setze die Richtung Vorwärts = LOW, Rückwärts = HIGH
267     digitalWrite(stepPin, HIGH);  // Gebe einen Schritt aus
268                                   // Definiert die Flussrate: 835 delay time entspricht 5µl/min bei der 5ml-Spritze, 1670
    delay time entspricht 2,5µl/min bei der 5ml-Spritze
269     delay(1670);                  // Warte ... Millisekunden
270     digitalWrite(stepPin, LOW);   // Stoppe den Schritt
```

```
271   }
272   updateMenu();
273 }
```

8.3 Preparation of Alkaline Phosphate Buffer (APB)

Alkaline Phosphate Buffer (APB)
100mM Tris (hydroxymethyl)aminomethane (Tris) ph 9,5
50mM Magnesium Chloride ($MgCl_2$)
100mM Sodiumchloride (NaCl)
0,1 % Tween 20

8.4 List of parts for syringe pump manufacturing

Product name	Manufac-turer	Seller	Pieces	Price €
Stepper-Driver WJMY A4988	WJMY	Amazon	1	2,03
Teensy 4.1 Mikrocontroller	PJRC	Conrad	1	51,99
Nema 17 Steppermotor 0,9° 2,4A	Joy-it	Conrad	1	31,99
Fine Hex Adjuster 1/4"-80, 4" long, F25SS400		Thorlabs	1	4,85
Locking Phosphor Bronze Bushing with Nut 1/4"-80, l=0,50"		Thorlabs	1	10,22
Universal Coupling Body		Technobots		3,91
Copper Clad Stripboard 160x100mm		Conrad		4,79
Screws M3x50		Conrad	3	13,47
Screws M3x25		Conrad	4	0,4
Muttern M3		Conrad	12	0,5
Micro-USB Cable		Conrad	1	2,99
Power Supply 19V		Conrad	1	24,99
Silver Steel 6mm x 333mm		Technobots	4	14,22
Zinc Collets 6mm pk/4		Technobots	12	6,63
Bearing LM6UU 6mm Bushing		Technobots	4	3,36
PMMA Plate			2	5
OLED 0,96 Zoll	AZDelivery	Conrad	1	7,99
Miniatur Taster	Youmile	Conrad	9	1,98
Socket Board 1pol 16row		Conrad	4	13,74
			Total:	205,05